

POLITECNICO DI TORINO

Corso di Laurea in Mechanical Engineering

Tesi di Laurea Magistrale

Stiffness reduction caused by vibration fatigue

Simulation of crack growth by VCCT under non linear response
vibration



Relatore

Prof. Stefano Marchesiello

Correlatore:

Prof. Dario Di Maio

Mauro FILONI

matricola: 241849

ANNO ACCADEMICO 2018 – 2019

Summary

This thesis deals with the fatigue behaviour of a composite laminate under bending cyclic load.

It is provided an initial theoretical introduction on how fracture in composite materials behave, with particular attention on the phenomena of "delamination", which will be the object of the software simulation in the second part of the thesis. The dissertation will guide the reader through the modelling of the laminate on a finite element software named Abaqus, focusing on modal dynamics theory and non linear dynamics.

Since the composite laminate requires too much computation time, a steel laminate is considered in the simulation with the crack opening path pre defined in order to simulate the delamination phenomena. Furthermore there will be considered different stiffness condition for the specimen. In particular a comparison between linear stiffness and non linear stiffness behaviour during the crack opening will be taken into account.

In the end all the results are collected with relative interpretations.

Acknowledgements

A volte ti ritrovi a dover scrivere il finale ancor prima di iniziare, o almeno questa è la sensazione che sto provando adesso, mentre scrivo queste righe. Sembra ieri il giorno in cui per la prima volta ho messo piede in aula universitaria, approcciandomi ad una disciplina che per molti versi sapevo essere nelle mie corde, ma che, almeno nel primo periodo, faticavo a comprendere a pieno. Col tempo i dubbi che mi assalivano svanirono quasi del tutto ed in pochi mesi la convinzione di aver fatto la scelta giusta si rafforzò. Tuttavia mentirei se dicessi che le mie insicurezze non sono mai tornate a tormentarmi, ed è proprio in quei momenti che ho trovato affidamento nelle persone che mi stavano accanto, è anche merito loro se sono arrivato a questo traguardo. Per questo motivo ci tengo a ringraziare uno per uno coloro che per me hanno significato davvero una spinta ad andare avanti, a non mollare mai.

Il Grazie più grande va ai miei genitori. Mamma e Papà, so di esservi costato davvero molto e non solo in termini economici, il mio pessimo umore durante le sessioni d'esame era fin troppo contagioso, ma ciò che più di tutto sento di dovervi è il tempo non speso insieme. So che siete orgogliosi di me e spero che questo mio successo vi ripaghi, seppur in minima parte, di tutto ciò che avete fatto per me.

Grazie a Martina, la mia ragazza. Hai sempre creduto in me e mi sei stata vicina anche e soprattutto nei momenti in cui la mancanza di casa si faceva sentire più forte. Anche a te so di aver chiesto tanto non essendo sempre presente fisicamente, ma tu hai compreso e mi hai appoggiato comunque, e per questo non posso che essertene grato.

Grazie ai miei nonni, da sempre un sostegno e una guida, uno dei motivi che mi ha spronato a fare sempre meglio senza risparmiarmi. L'orgoglio che leggo nei vostri occhi mi ripaga di tutte le fatiche spese finora.

Grazie a Luigi, che fossi vicino o lontano non passava giorno che non ci sentissimo e questo mi ha fatto sentire meno distante da casa; il fatto di sapere di poter contare su un amico come te per me è stato motivo di forza e orgoglio.

Infine ci tengo a ringraziare tutti gli amici e i parenti che in questi anni ho avuto accanto e senza i quali tutti i percorsi affrontati sarebbero stati di sicuro più ripidi e insidiosi. Per questo motivo dedico questa tesi a tutti voi, consapevole del fatto che sia solo un rito di passaggio da ciò che è stato il percorso universitario a qualcosa di ignoto, ma potenzialmente ugualmente stimolante e ricco di soddisfazioni.

Contents

List of Tables	7
List of Figures	8
I First Part	13
1 Introduction	15
2 Fatigue overview	17
2.1 Introduction	17
2.2 Crack initiation	18
2.3 Crack propagation	20
2.3.1 Modes of fracture	20
2.3.2 Crack growth as a function of ΔK	21
2.3.3 Paris' law	22
2.3.4 Short crack	24
2.4 Delamination in composite	24
3 F.E.M. applied to the studied case	29
3.1 Beam element	29
3.1.1 Free-free beam theory	29
3.1.2 Abaqus model	34
3.2 Crack propagation prediction with FEM	36
3.2.1 Crack closure method	36
3.2.2 Virtual crack closure technique (VCCT)	38
3.3 Non linear dynamics	40
3.3.1 Duffing Equation	41

II	Second Part	45
4	Abaqus model	47
4.1	The problem of rigid body motion	47
4.1.1	Results	49
4.2	Damping in Abaqus	51
4.3	Matlab automatization	52
4.4	Cohesive elements	54
4.5	Final model (Case 1)	61
4.5.1	Procedure for crack growth evaluation	64
4.5.2	Results	68
4.6	Final model (Case 2)	74
5	Conclusions	79
5.1	Future work	80
6	Matlab code	81
	Bibliography	87

List of Tables

3.1	Beam properties	30
3.2	Wave numbers for modes	32
4.1	Rayleigh parameters	51

List of Figures

1.1	Sequence showing the growth of a crack from a 90° ply into a 0° ply in a graphite epoxy laminate. [11]	15
2.1	Stresses at notch level	18
2.2	Typical SB crack in fatigued monocrystal Cu	19
2.3	Fatigue cracks initiated from GBs for copper bicrystals.	19
2.4	Example of fatigue crack initiation due to inclusions	20
2.5	Fracture modes	21
2.6	Crack growth rate as function of ΔK	22
2.7	Comparison between theoretical and approximated Crack growth rate curve	23
2.8	Iteration for choosing the correct amount of Δa [5].	25
2.9	Schematic representation of delamination phenomena	26
2.10	Transversal load	26
2.11	Notch	27
3.1	Beam element 270x2 mm	29
3.2	Equilibrium at an infinitesimal beam element	30
3.3	Mode shapes	33
3.4	First natural frequency mode shape	34
3.5	Load applied on the laminate	34
3.6	Frequency response function in x_0	35
3.7	Vertical displacement of x_0 over time	35
3.8	Crack closure method a) First step: crack closed and b) second step: crack extended.	37
3.9	One step VCCT	38
3.10	Crack with one dimensional discontinuity. (a) Non deformed. (b) Deformed	39
3.11	Spring mass system	40
3.12	Non linear spring mass system	41
3.13	$f(x)$ at different μ [8]	43

3.14	Non linear Displacement-frequency plot, comparison between hardening and softening behaviour [13]	43
4.1	System with load	47
4.2	Linear perturbation steps	48
4.3	Displacement of x_0	49
4.4	Model with pinned nodal points	49
4.5	Displacement comparison	50
4.6	Stress comparison	50
4.7	Zoom on the crack site, set of nodes "Node1"	52
4.8	Zoom on the crack site, set of nodes "Node2"	52
4.9	Zoom on the crack site, set of nodes "Node3"	53
4.10	Zoom on the crack site, set of nodes "Node4"	53
4.11	Zoom on the crack site, set of nodes "Node5"	53
4.12	Edges considered in the interactions	54
4.13	Point considered to take data x_1	55
4.14	Displacement of point x_1 in linear case	55
4.15	Deformation at crack iniization	56
4.16	Displacement of point x_3 and x_2	56
4.17	Non linear stiffness	57
4.18	Displacement of point x_1	58
4.19	Fast Fourier transform of linear stress in x_1	59
4.20	Vertical stress at point x_1	60
4.21	Vertical stress at point x_1 in both linear and non linear case	60
4.22	New crack path	61
4.23	Zoom on the springs on the crack path	62
4.24	Non linear spring characteristic	63
4.25	Zoom on the crack	64
4.26	Displacement in time at point x_2	65
4.27	Force in time at point x_1	65
4.28	Difference between the displacement of point x_2 and point x_3	66
4.29	External load in time	67
4.30	Crack growth rate comparison	68
4.31	Comparison between FFT of the linear and non linear case	69
4.32	FFT of non linear case	70
4.33	Third, fifth and seventh multiple of the main harmonic	71
4.34	First harmonic during crack propagation	72
4.35	First and third harmonic during crack propagation	72
4.36	Buckling in compression	73
4.37	Tensional behaviour	73

4.38	Tensional behaviour without contact	73
4.39	Model with springs	74
4.40	Crack growth rate comparison (case 2)	75
4.41	Fast Fourier Transform of the force with non linear spring (case 2)	76
4.42	Crack growth rate comparison (case 2)	77

If you want to find the secrets of the universe, think in terms of energy, frequency and vibration.

[N. TESLA]

Part I
First Part

Chapter 1

Introduction

It is very important for structural engineers understanding how composite materials fails, for this reasons a lot of expensive and long time test have been taken out during years.

By considering a composite laminate which undergoes a bending cyclic stress, it is found out that the delamination is one of the main failure mechanism of composite materials; the crack opens along the transversal direction of the specimen, but at a certain point it change the propagation direction and continue along the longitudinal one. An example is shown in fig. 1.1.

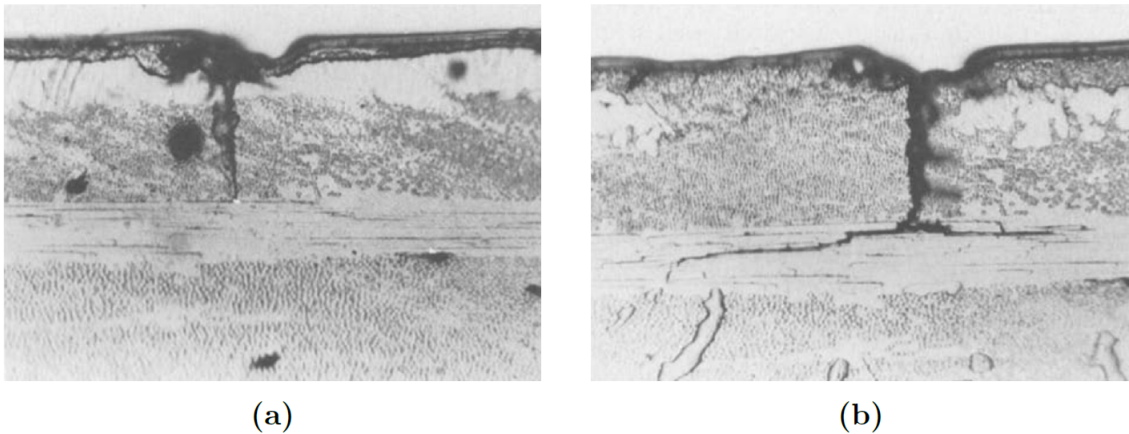


Figure 1.1. Sequence showing the growth of a crack from a 90° ply into a 0° ply in a graphite epoxy laminate. [11]

It is this type of behaviour the research object of this thesis, in particular the scope is to provide a comparison between the crack opening in time of

a laminate which undergoes a cyclic bending load with a frequency equal to the first natural frequency of the specimen (so trying to excite only the first mode) in two different stiffness conditions: linear and non linear one. To do so, in the first part of this thesis, there will be provided:

- several theoretical information about the fatigue mechanism, pointing out what happens in composite materials;
- the comparison between results obtained from modal analysis by hand and by software;
- the methodologies to face the problem by finite element analysis;

In the second part there will be shown all the operative passages followed in order to reach the final scope, including the data post processed by Matlab. Nevertheless, in order to simplify the model and so reducing the computation time, a steel laminate is considered instead of a composite one, with the crack path pre specified in order to simulate the delamination behaviour.

Chapter 2

Fatigue overview

2.1 Introduction

It is very common to find machine members, which undergo cyclic or repeated load, completely or partially failed although the stress was even significantly lower than the ultimate strength of the material.

This phenomenon appears after a high number of cycles; for this reason this type of failure is called "Fatigue failure".

The American Society for Testing and Material (ASTM) gives the following definition of Fatigue [1]:

“The process of progressive localized permanent structural changes occurring in a material subjected to conditions that produce fluctuating stresses at some point or points and that may culminate in cracks or complete fracture after a sufficient number of fluctuations.”

This type of failure begins with a small crack; it usually appears at discontinuities of the material like a notch or a hole. Then the concentrated stresses increase locally and the crack grows up until the portion of remained material is unable to sustain the load and it fails suddenly.

To summarize, it is possible to identify three main moments in the crack evolution.

- Crack initiation

- Crack propagation
- Fracture

2.2 Crack initiation

Crack initiation, as the whole fatigue process, depends by cyclic plastic deformation.

Moreover, as it can be demonstrated by a lot of experimental observation, in a homogeneous flaw-free material microcracks originate at free surface level; probably it is due to the fact that stresses are significantly higher close or at the surface [2].

In a large number of engineer component the higher stress at the surface is due to notches, which experience stress values exponentially higher respect to the rest of the material (fig. 2.1).

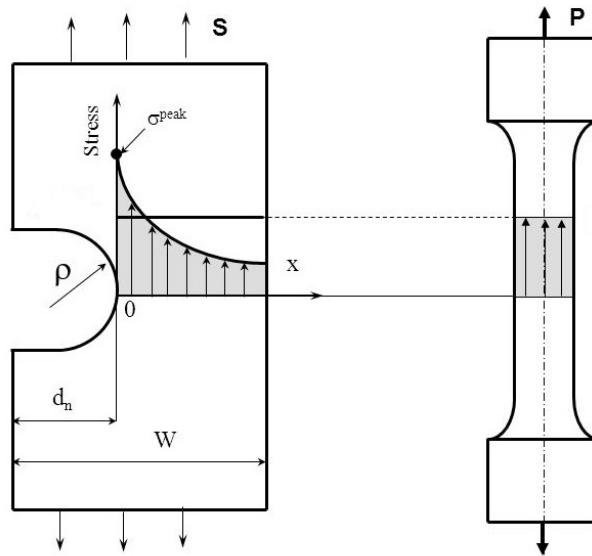


Figure 2.1. Stresses at notch level

Over macroscopic sources of stress concentration there are even microscopic stress concentrators, for instance micro grooves due to machining, surface step caused by dislocations and presence of second-phase particles.

It could be of interest analyzing some of the most common type of crack initiation.

- **Initiation at Persistent Slip Bands:** it happens that, in pure metal and some alloys, irreversible dislocation slides under cyclic load leading to the development of persistent slip bands. An example of this type of initiation is shown in fig. 2.3.

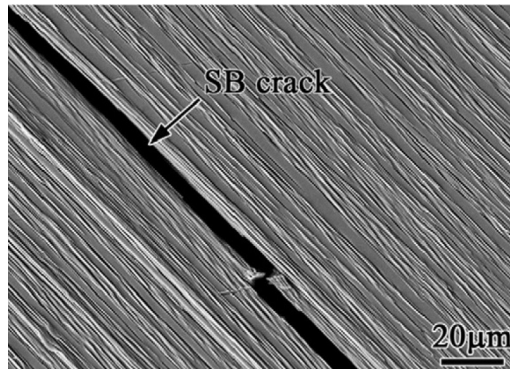


Figure 2.2. Typical SB crack in fatigued monocrystal Cu

- **Initiation at Grain Boundaries:** Initiation at grain boundaries is also conditioned by the cyclic slip processes. The first micro-crack is usually caused by slip impingement which in turn causes stress concentration at grain boundaries level. The initiation site is commonly located in a cluster of grains with similar crystallographic orientation which make easier the slip transmission.

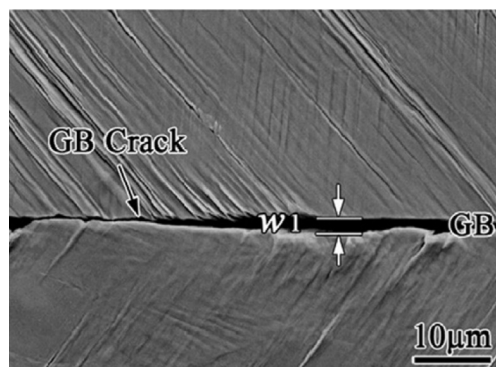


Figure 2.3. Fatigue cracks initiated from GBs for copper bicrystals.

- **Initiation at Inclusions:** this type of initiation occurs when there are large enough particles in the material. Fatigue crack preferentially tends to initiate at the second-phase particles for the specimens with relatively small grain size; the reason is probably that they are less tough than big ones. An example can be seen in fig. 2.4

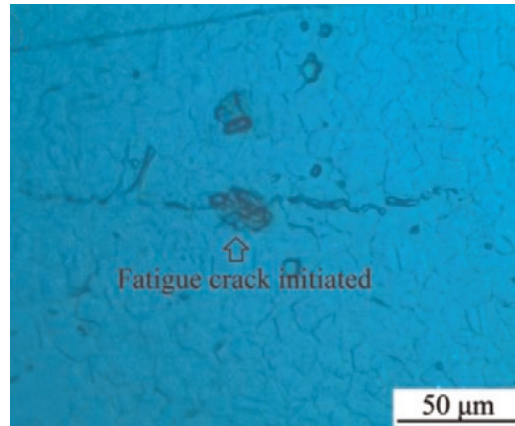


Figure 2.4. Example of fatigue crack initiation due to inclusions

2.3 Crack propagation

This step of the failure mechanism is fairly difficult to be predicted, so many models have been developed in order to obtain an approximated model of the material behaviour.

When the crack is small it interacts with microstructure and it is analyzed by continuum mechanics approaches [3]. Instead, when the crack gradually grows, it starts to be insensitive to microstructure and analysis are performed by fracture mechanics models.

2.3.1 Modes of fracture

Consider a cracked plate, there are several manners in which the crack may propagate when a force is applied to the plate [4]. In fig 2.5 are shown the three different fracture modes.

In the *Mode I*, or opening mode, the plate is loaded by tensile forces and the deformations are symmetric with respect to the planes perpendicular to

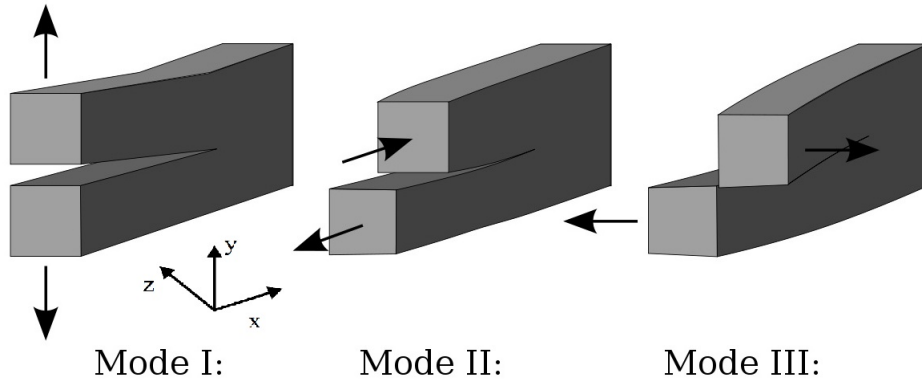


Figure 2.5. Fracture modes

the y axis and the z axis.

In the *Mode II*, or sliding mode, the plate undergoes shear forces parallel to the crack surfaces, which slide over each other in the x direction. Deformations are symmetric with respect to the plane perpendicular to the x axis and skew symmetric with respect to the plane perpendicular to the y axis.

Finally, in the *Mode III*, or tearing mode, the plate is loaded by shear forces parallel to the crack surfaces, they slide over each other in the z direction. The deformations are then skew-symmetric with respect to the plane perpendicular to the z and the y axis.

2.3.2 Crack growth as a function of ΔK

In static loading the stress intensity factor K_I depends on the static stress σ and on the geometry of the specimen. For example, if the stress is kept constant, the fracture will take place at a certain crack length $a = a_C$ at which corresponds a stress intensity factor $K_I = K_{IC}$; for $a < a_C$, and so $K_I < K_{IC}$ the crack will not propagate.

In dynamic loading the fracture happens if $K_I = K_{IC}$, but it can even take place if $K_I < K_{IC}$ because the crack may still propagate.

During experiment the crack growth is measured as a function of the stress intensity factor; as can be seen in fig 2.6 there can be distinguished three main regions:

- **Region I:** it is possible to see that, under a certain value of ΔK , the crack will not propagate. When ΔK is too small there are so many variables that affect the prediction, they depend on microstructure and flow properties of the material.
- **Region II:** the crack growth rate, almost insensitive to the microstructure in this step, is linearly dependent by the stress intensity factor until it reaches the fracture toughness at K_C and the material will fail. One of the possible method to predict the material behaviour in this region is the Paris' law, which will be in-depth investigated in sec. 2.3.3.
- **Region III:** The crack growth rate accelerate and finally fracture will occur.

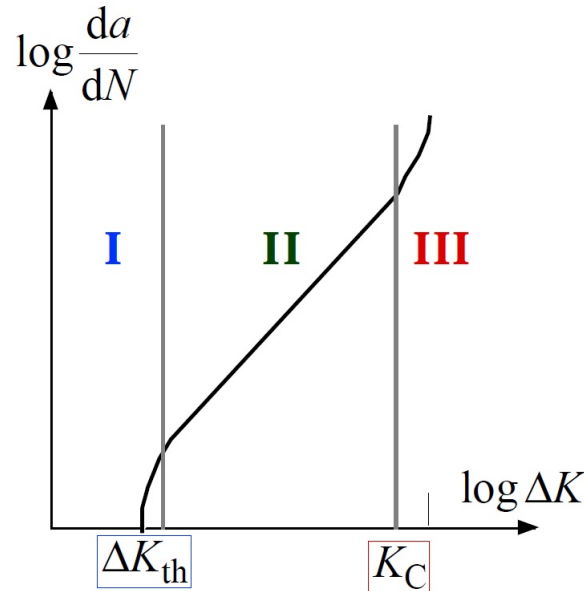


Figure 2.6. Crack growth rate as function of ΔK

2.3.3 Paris' law

As anticipated in sec. 2.3.2, one of the most used method to predict the crack growth rate is the Paris' law. In fig. 2.7 is represented the typical relationship between the crack growth rate and the range of the stress intensity factor.

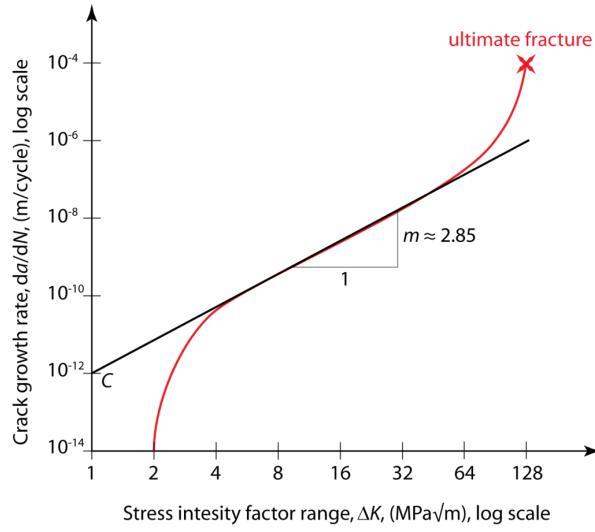


Figure 2.7. Comparison between theoretical and approximated Crack growth rate curve

In practice, the Paris law is calibrated to model the linear interval around the center.

The equation at the base of the Paris' Law is the following equation.

$$\frac{da}{dN} = C\Delta K^m \quad (2.1)$$

Where:

a : dimension of the crack

N : number of cycles

C and m : Constants dependent on the material

ΔK : difference between maximum and minimum stress strain rate.

The estimation of fatigue life [5] can be made by integrating the 2.1.

$$\int_{N_0}^{N_f} dN = \int_{a_0}^{a_f} \frac{da}{C\Delta K^m} \quad (2.2)$$

The 2.2 can be used to determine either the number of cycle $N_f - N_0$ required to take the crack from a_0 to a_f , or how large is the crack after an arbitrarily number of cycle. Unfortunately is very complicated to obtain an analytical relation between a and N , mainly due to ΔK which is function

of both the crack geometry and stress during the experiment. For this reason a numerical method is more suitable for computation, so the following equations have been introduced.

$$N_{n+1} = N_n + \frac{\Delta a}{C[\Delta K(a_n)]^m} \quad (n = 0, 1, \dots, N) \quad (2.3)$$

$$a_{n+1} = a_n + C[\Delta K(a_n)]^m \Delta N \quad (n = 0, 1, \dots, N) \quad (2.4)$$

In Eq. 4.13 the crack growth increment Δa is taken as a constant, lower will be taken the value of Δa and higher will be the integration accuracy. Obviously, taking an infinitesimal Δa , the solution should converge to the exact one; however there is an iterative process to properly choose Δa and it is represented in fig. 2.8. The accuracy level is expressed by a certain tolerance ε .

The main drawbacks of the Paris' law are that it does not take into account the mean stress effect and the history effects; further it is only valid in conditions with uniaxial loading and strictly for large cracks.

2.3.4 Short crack

It is worth, for completeness, to spend several words about the short crack behaviour.

$$\frac{da}{dN} = f(\Delta K) \quad (2.5)$$

So far the equation used is dependent by ΔK (Eq. 2.5). However ΔK in turn depends by the amplitude of the normal stress, but short cracks are shear stress driven and so the model mentioned before is not valid. There can be distinguished two types of short cracks:

- **mechanically short cracks:** compared with large cracks with same ΔK they propagate faster
- **microstructurally short cracks:** they interact closely with the microstructure and grow fast.

2.4 Delamination in composite

Failure analysis of laminated composite has become a very important field of study with the relatively recent increasing of composite applications. In

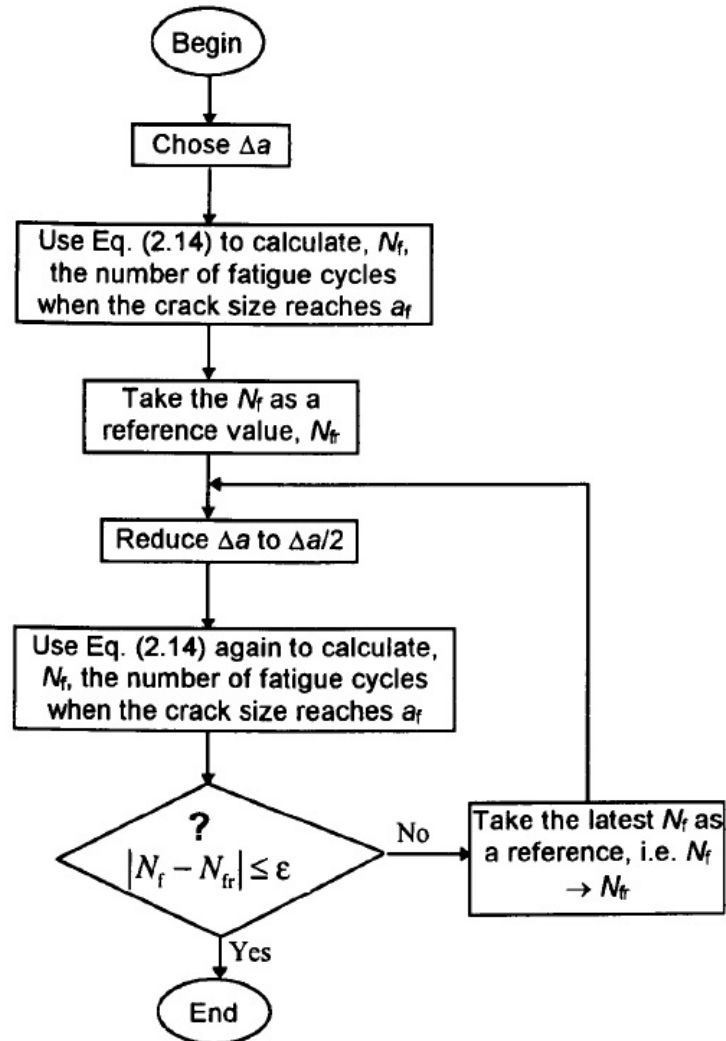


Figure 2.8. Iteration for choosing the correct amount of Δa [5].

particular the Delamination [7], separation of two adjacent layers due to weakening interface layer between them, represents the most critical failure mode in composite.

Basically, delamination in laminated composite can develop in every of the three fracture modes (2.5) or a combination of them. The energy required to initiate delamination in the material is referred to the "critical strain energy release rate", indicated with G_c . This value depends by the delamination mode, in fact there are three values of G_c for the three modes respectively:

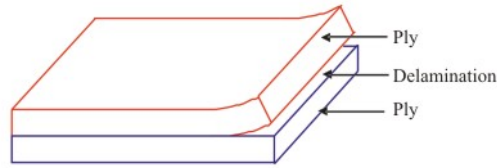


Figure 2.9. Schematic representation of delamination phenomena

G_{1c} , G_{2c} and G_{3c} . The critical strain energy release rate is affected by different parameters: fibre volume fraction, ply orientation, material properties such as tensile strength and elastic modulus of the resin and the fibre.

The main causes of delamination are:

- **Manufacturing defects:** improper laying of laminae, insufficient curing parameters (temperature, duration and pressure), air pockets and inclusions.
- **Transverse stresses generated by load:** since the interface is weaker than layers for what regards transverse strength, its failure is transverse stresses dominated.

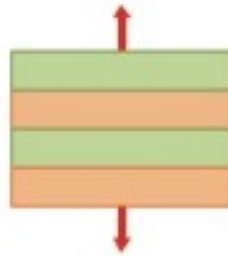


Figure 2.10. Transversal load

- **Laminate geometry:**
 1. **Free edges:** at free edges level transverse normal and shear stresses are very high.
 2. **Notch:** The notch act as a crack, in its proximity there is a high three-dimensional stress state.
 3. **Cut-out:** Cut-out boundaries behave as free edges and so in this zone the transverse stresses are significant.

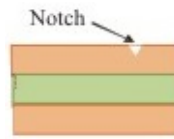


Figure 2.11. Notch

4. **Bounded joint:** if bonding is not done properly this may lead to weaker joints, and so delamination can take place.
5. **Ply drop:** The ply termination is a high stress region for neighboring laminae, this can cause delamination of the plies adjacent to the ply drop region.

Delamination is dangerous because strength and stiffness are reduced; stress concentration in load bearing plies leading to a rapid growth of delamination which ends in the failure of the laminate.

Chapter 3

F.E.M. applied to the studied case

3.1 Beam element

The objective of this thesis is the study of the fatigue behaviour of a laminate; so, in this section, basic knowledge of continuum dynamics related to the model which will be studied are introduced.

The laminate is considered as a beam, so it will be investigated the dynamic behaviour of a free-free beam. The study is performed on a mild steel specimen (Fig. 3.1), which properties are reassumed in Tab.3.1.



Figure 3.1. Beam element 270x2 mm

3.1.1 Free-free beam theory

From the equilibrium equation of an infinitesimal element of the beam (Fig. 3.2) They are obtained the following equations, the first one from translation equilibrium and the second one from rotation equilibrium.

Data	Value	Unit of measure
Width	270	mm
Height	2	mm
Young modulus (E)	210	MPa
Density (ρ)	7800	kg/m^3
Damping ratio ζ	0.04	-
Moment of inertia I_y	$6,67 \cdot 10^{-14}$	m^4

Table 3.1. Beam properties

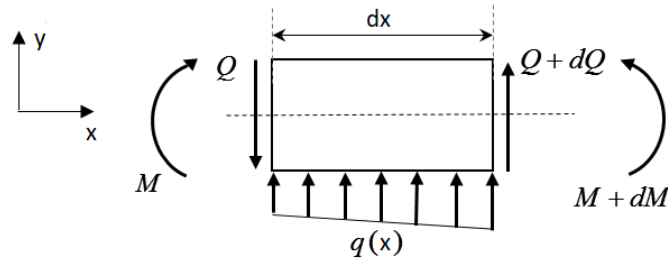


Figure 3.2. Equilibrium at an infinitesimal beam element

$$\rho A \frac{\partial^2 y}{\partial t^2} = \frac{\partial Q}{\partial z} + q(z) \quad (3.1)$$

Where:

ρ : Density

A : Cross section area

Q : Shear force

$q(z)$: Distributed forces

$$Q + \frac{\partial M}{\partial z} + q(z) = 0 \quad (3.2)$$

Where:

M : Moment

For a beam the moment is equal to:

$$M_z = EI_y \frac{\partial'' y}{\partial z^2} \quad (3.3)$$

Where:

E : Young modulus

I_y : Moment of inertia along y axis

So, neglecting the distributed load $q(z)$, the equation so obtained is:

$$\rho A \frac{\partial'' y}{\partial t^2} + EI_y \frac{\partial^{IV} y}{\partial x^4} = 0 \quad (3.4)$$

From the Eq. 3.4 it is possible to obtain the first natural frequency by the following formula:

$$\omega^2 = \frac{EI_y k^4}{\rho A} \quad (3.5)$$

Where β is the wavenumber. From Tab.3.2, for mode 1, k is equal to 17.5. Substituting the values in Tab. 3.1:

$$\omega_1 = \sqrt{\frac{EI_y}{\rho A} k^4} = \sqrt{\frac{210 * 10^9 * 6,67 * 10^{-14}}{7800 * 2 * 10^{-7}} 17,5^4 \frac{rad}{s}} = 919 \frac{rad}{s} = 146 Hz \quad (3.6)$$

The displacement of every beam point from now on will be called $u(x, y, z, t)$, in particular, since it is a beam, the interest is mainly focused on the y behaviour, so it will be considered only the displacement along y $u(x, t) = u_y$.

$$u_y = v(x)\eta(t) = 0 \quad (3.7)$$

In Eq. 3.7 u_y has been split considering two parts, one dependent from the x coordinate and the other one time dependent. From 3.1 and 3.7 it is possible to derive the shape of both spacial and time components:

$$v(x) = C_1 \sin(kx) + C_2 \cos(kx) + C_3 \sinh(kx) + C_4 \cosh(kx) = 0 \quad (3.8)$$

$$\eta(t) = \cos(\Omega t + \varphi) = 0 \quad (3.9)$$

C_1, C_2, C_3 and C_4 are constants which can be calculated defining the boundary conditions, Ω is the excitation frequency and φ is the phase.

In a free free beam, from shear forces and moment equilibrium, the following boundary conditions can be setted:

$$\begin{cases} v''(0) = 0 \\ v'''(0) = 0 \\ v''(L) = 0 \\ v'''(L) = 0 \end{cases} \quad (3.10)$$

and so:

$$\begin{cases} -C_2 + C_4 = 0 \\ -C_1 + C_3 = 0 \\ -C_1 \sin(kL) - C_2 \cos(kL) + C_3 \sinh(kL) + C_4 \cosh(kL) = 0 \\ -C_1 \cos(kL) + C_2 \sin(kL) + C_3 \cosh(kL) + C_4 \sinh(kL) = 0 \end{cases} \quad (3.11)$$

The system can be rearranged in matrix form as:

$$\begin{bmatrix} \sinh(kL) - \sin(kL) & \cosh(kL) - \cos(kL) \\ \cosh(kL) - \cos(kL) & \sin(kL) + \sinh(kL) \end{bmatrix} \begin{Bmatrix} C_1 \\ C_2 \end{Bmatrix} = \begin{Bmatrix} 0 \\ 0 \end{Bmatrix} \quad (3.12)$$

In order to obtain a non trivial solution, the determinant of 3.12 must be null; so the following equations is obtained.

$$\cosh(kL)\cos(kL) = 1; \quad (3.13)$$

The Eq.3.13 can be numerically solved to obtain:

Mode n°	$k_n \mathbf{L}$
0	0
1	4.73
2	7.8532
3	10.9956
4	14.1371

Table 3.2. Wave numbers for modes

Substituting the values so obtained in 3.11 it is possible to extrapolate the mode shapes from the following:

$$v(x) = [\sinh(k_n x) + \sin(k_n x)] + \frac{\sin(k_n L) - \sinh(k_n L)}{\cosh(k_n L) - \cos(k_n L)} [\cosh(k_n x) + \cos(k_n x)] \quad (3.14)$$

Simply changing the values of k_n from Tab. 3.2 they are obtained the different mode shapes.

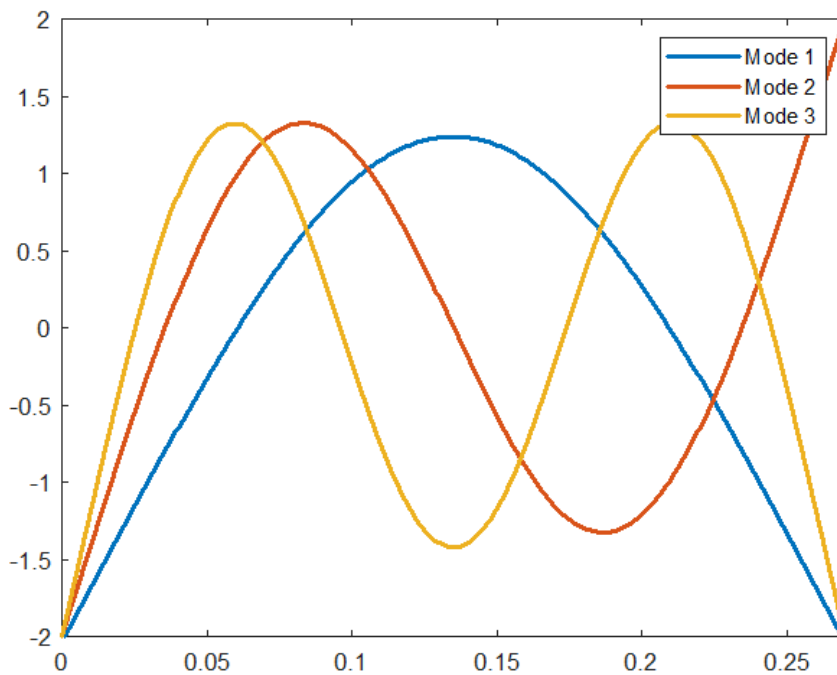


Figure 3.3. Mode shapes

3.1.2 Abaqus model

The model discussed in the previous section has been modelled in Abaqus, a finite element software which performs both static and dynamic analysis.

Firstly the first natural frequency and the respective mode shape has been taken out.

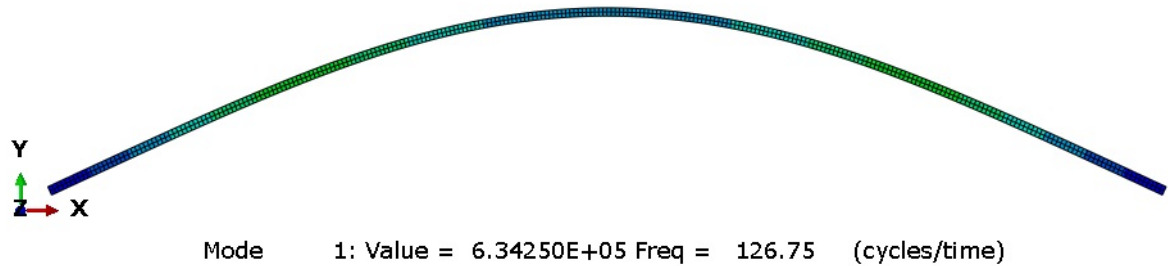


Figure 3.4. First natural frequency mode shape

As can be seen in Fig. 3.4, the value of the first natural frequency is very similar to the one obtained in Sec. 3.1.1 with the 3.5. In order to compute the Frequency response function of the displacement at the point x_0 (a node in the middle upper part of the specimen), a force of 1 N is applied as shown in figure 3.5 and, through the "steady-state dynamics Modal" step in Abaqus, the plot in Fig. 3.6 is obtained.



Figure 3.5. Load applied on the laminate

As expected the peak of the response is at around 130 Hz. The next step is to apply a harmonic force in the same point but with a frequency equal to the resonance one; in this way the "Modal Dynamic" step will take out the displacement in time of point x_0 (Fig 3.7).

It is worth to note that, even if at resonance, the system reaches the steady state conditions; this is due to the damping assigned to the model, without

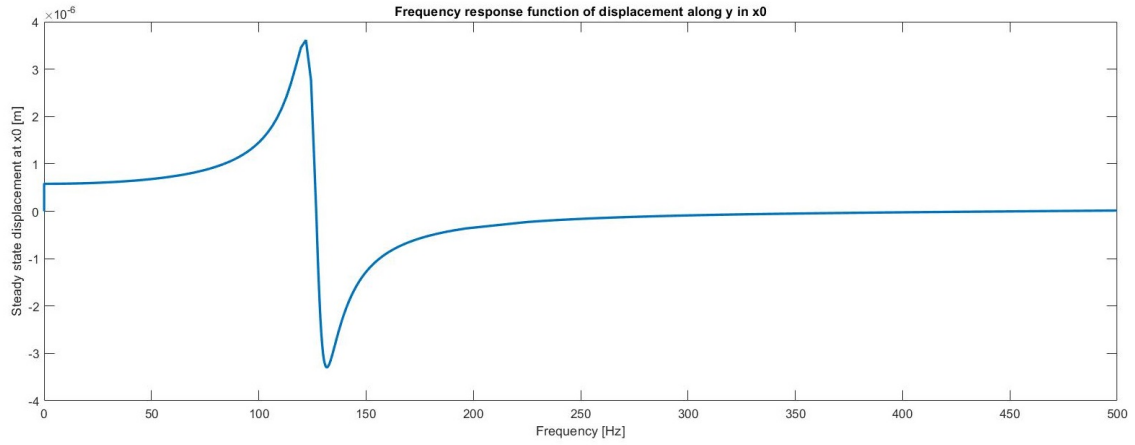


Figure 3.6. Frequency response function in x_0

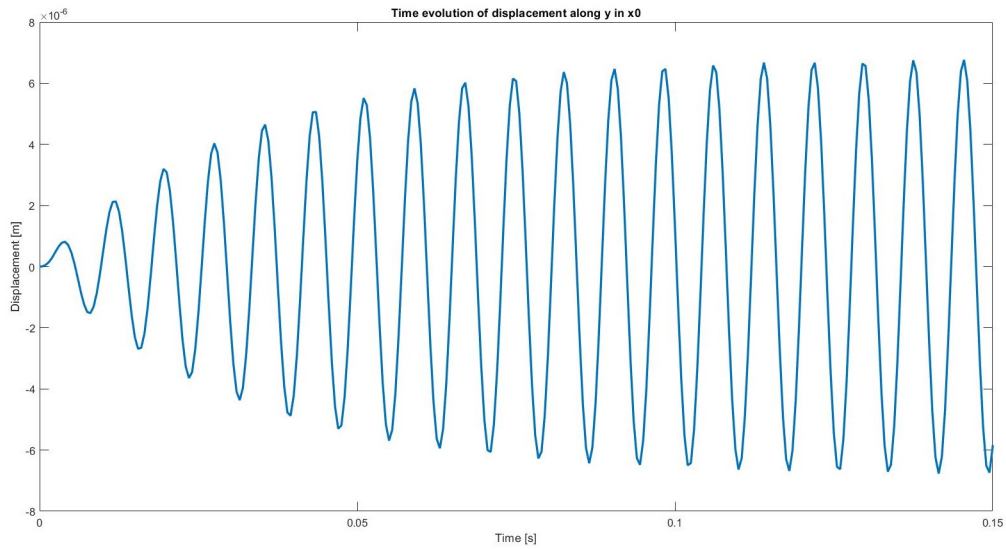


Figure 3.7. Vertical displacement of x_0 over time

it the amplitude of the oscillations would theoretically increase linearly to infinite.

3.2 Crack propagation prediction with FEM

As discussed in sec. 2.4, delamination is one of the most common failure modes of composite laminate. The growth of the crack derive by a mixity of mode I, II and III and depends by some parameters that have to be defined:

- G_T : Total strain energy release rate
- G_I : Mode I component of SERR due to interlaminar tension
- G_{II} : Mode II component of SERR due to interlaminar sliding shear
- G_{III} : Mode III component of SERR due to interlaminar scissoring shear
- G_c : Interlaminar fracture toughness

When, for instance, $G_{II}/G_T = 1$ it is expected a mathematical relationship between G_c and G_{II}/G_T ; failure will take place when the total energy release rate G_T exceeds the interlaminar fracture toughness G_c .

To compute the strain energy release rate, a lot of methods have been developed based on results obtained by finite element analysis [6].

3.2.1 Crack closure method

The *Crack closure method*, to not be confused with the *Virtual crack closure technique*, consists in two finite element analysis step in which the crack is physically extended, or closed (Fig. 3.8)

This method is based on Irwin's crack closure integral; it is based on the assumption that the energy ΔE released extending the crack fro a to $a + \Delta a$ is equal to the energy required to close the crack between location l and i . Index 1 and 2 are referred respectively to Fig. 3.8(a) and 3.8(b); so, for a crack modeled with two-dimensional four noded elements the work needed to close the crack along one element side is equal to:

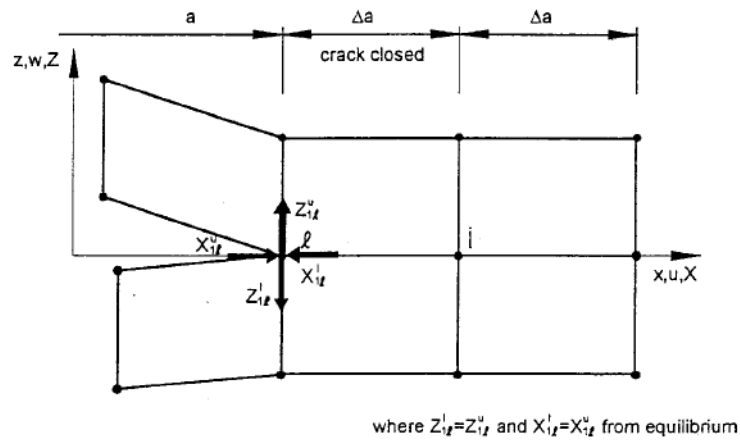
$$\Delta E = \frac{1}{2}[X_{1l}\Delta u_{2l} + Z_{1l}\Delta w_{2l}] \quad (3.15)$$

Where:

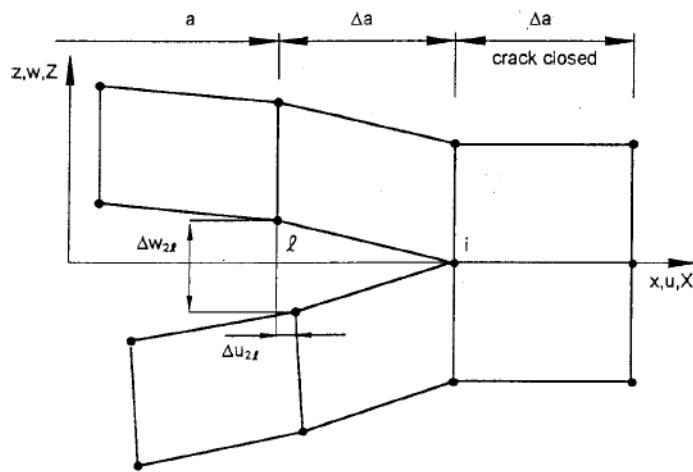
X_{1l} is the shear force

Z_{1l} is the opening force

Δu_{2l} difference in shear nodal displacement at node l .



(a). First Step - Crack closed



(b). Second Step - Crack extended

Figure 3.8. Crack closure method a) First step: crack closed and b) second step: crack extended.

Δw_{2l} difference in opening nodal displacement at node l .

Forces X_{1l} and Z_{1l} may be obtained in the first finite element analysis, when the crack is closed at node l ; while in the second analysis they may be obtained the values of displacement at the same node, but when the crack is open.

3.2.2 Virtual crack closure technique (VCCT)

Generalities

The *virtual crack closure technique* is based on the same assumption of the *crack closure method*, but with a small difference; it is assumed that the extension of a crack from $a + \Delta a$ to $a + 2\Delta a$ does not significantly alter the state at the crack tip.

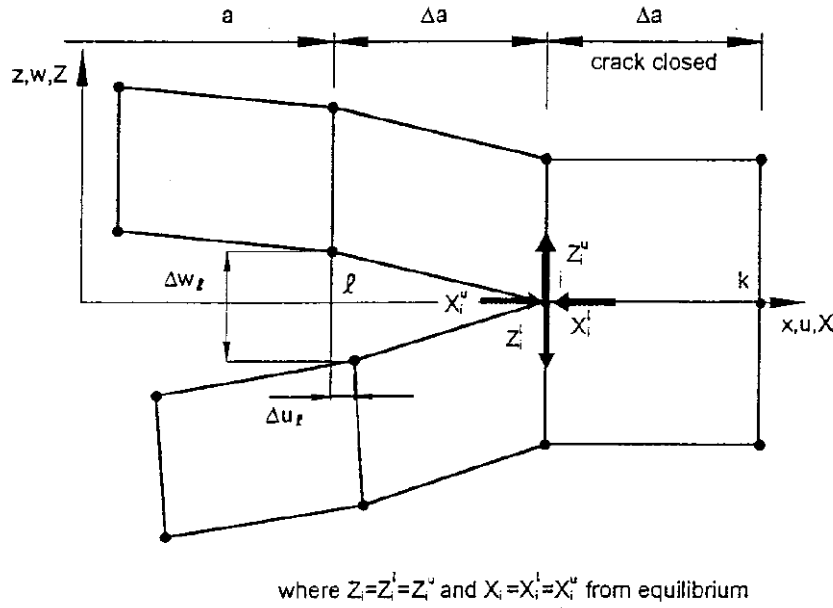


Figure 3.9. One step VCCT

So, referring to Fig. 3.9, when the crack tip is at node k , the displacements at node i are approximately equal to the displacements at node l when the crack tip is located at node i . It is possible to derive the energy required to close the crack along one element side:

$$\Delta E = \frac{1}{2}[X_i \Delta u_l + Z_i \Delta w_l] \quad (3.16)$$

Where

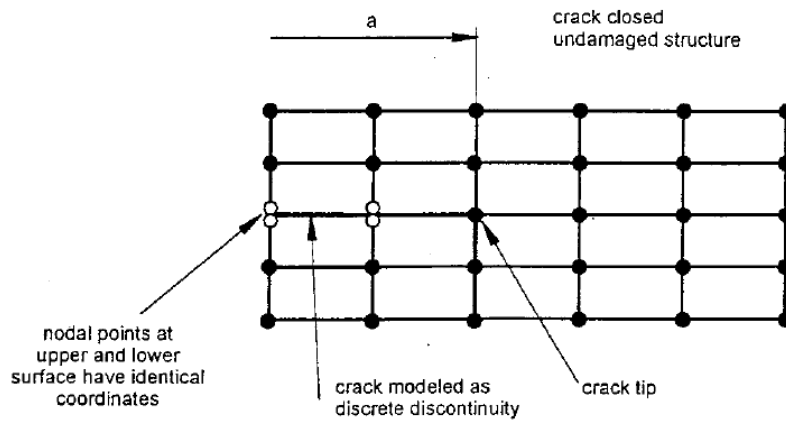
X_i is the shear force at nodal point i

Z_i is the opening force at nodal point i

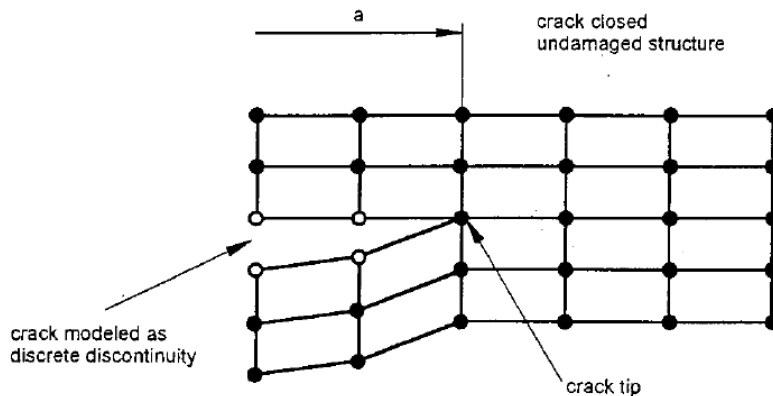
Δu_l and Δw_l are the shear and opening displacements at node l

Equations for two dimensional analysis

In a two dimensional finite element plane stress the crack is represented as a one dimension discontinuity between two lines of nodes (Fig. 3.10(a)). The nodes of the upper line have the same coordinates of the ones in the bottom line, but, once the crack is opened, detached nodes of a line are freely to move independently respect nodes in the other line (Fig. 3.10(b)).



(a). Initially modeled, undeformed finite element mesh



(b). Deformed finite element mesh

Figure 3.10. Crack with one dimensional discontinuity. (a) Non deformed. (b) Deformed

In the crack propagation analysis the nodes are sequentially released in order to make the crack growing "manually". The formulae used in the 2D analysis for the stress release rate are:

$$G_I = -\frac{1}{2\Delta a} Z_i(w_l - w_{l*}) \quad (3.17)$$

$$G_{II} = -\frac{1}{2\Delta a} X_i(u_l - u_{l*}) \quad (3.18)$$

These last values will be used into the Paris'law in order to obtain the crack growth rate.

3.3 Non linear dynamics

In linear dynamics, for a simple spring mass system (Fig. 3.11), the equation of motion is the 3.19.

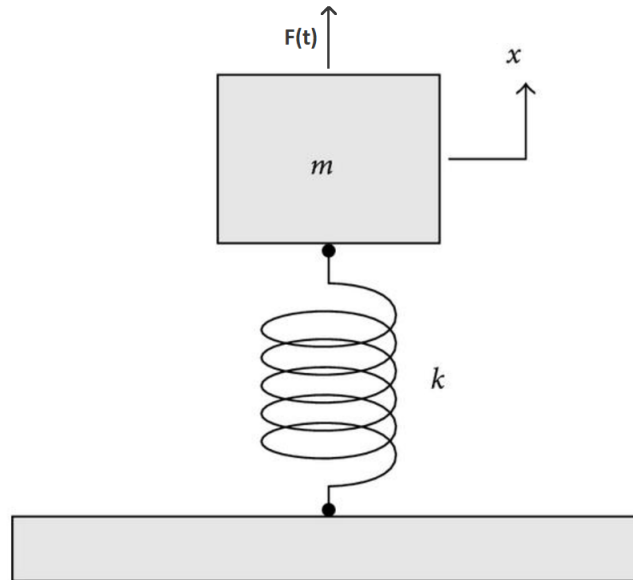


Figure 3.11. Spring mass system

$$m\ddot{x} + kx = F(t) \quad (3.19)$$

Where:

m is the mass

k is the stiffness

$F(t)$ is a harmonic load applied to the mass

x is the displacement of the mass

\ddot{x} is the acceleration of the mass

Some troubles comes out if the studied system is non linear, for instance the stiffness of the spring has a cubic behaviour instead of a linear one; the resulting equation will be the 3.20.

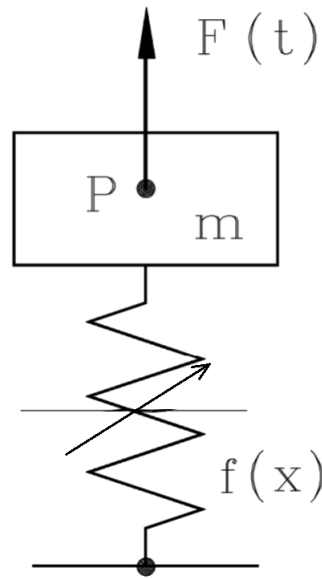


Figure 3.12. Non linear spring mass system

$$m\ddot{x} + f(x) = F(t) \quad (3.20)$$

Where $f(x)$ is different from the term kx of equation 3.19; practically it is the force of the non linear spring at different elongation, but it can be whichever type of equation, so not strictly linear. Supposing it is present even non linear damping the 3.20 becomes:

$$m\ddot{x} + \beta(\dot{x}) + f(x) = F(t) \quad (3.21)$$

Where $\beta(\dot{x})$ is the force due to non linear damping.

3.3.1 Duffing Equation

It is possible to develop $f(x)$ in Taylor series in order to obtain something like following.

$$f(x) = a_0 + a_1x + a_2x^2 + a_3x^3 + \dots \quad (3.22)$$

Where a_i (i from 0 to n) is the coefficient of the term of i^{th} order.

Let us assume a skew symmetric system without any translation a_0 , so the even terms disappear.

$$f(x) = a_1x + a_3x^3 + a_5x^5 + \dots \quad (3.23)$$

Since near to the 0 the higher order terms become too small it is worth to take into account only the first two terms of 3.23.

$$f(x) = a_1x + a_3x^3 \quad (3.24)$$

From the 3.24, substituting $k = a_1$ and $\mu = a_3/a_1$.

$$f(x) = kx(1 + \mu x^2) \quad (3.25)$$

Putting the 3.25 into the 3.20:

$$m\ddot{x} + kx(1 + \mu x^2) = F(t) \quad (3.26)$$

Plotting the behaviour of $f(x)$ at different μ , the following pattern is obtained.

It is possible to distinguish two main parts; in the first one $\mu > 0$ and it is defined hardening behaviour, while in the second one $\mu < 0$ and it is softening behaviour. For the purpose of this thesis μ will be considered higher than 0.

Since it has been assumed a skew symmetric $f(x)$, the solution of 3.26 could be expressed as follow:

$$x = x_1\sin(\omega t) + x_2\sin(3\omega t) + x_3\sin(5\omega t)\dots \quad (3.27)$$

Only odd terms appears in the solution, so it depends only by the odd multiple of the forcing frequency. In the final chapter this result will appear more clearly, thanks to the FFT which will put in evidence all the harmonics involved.

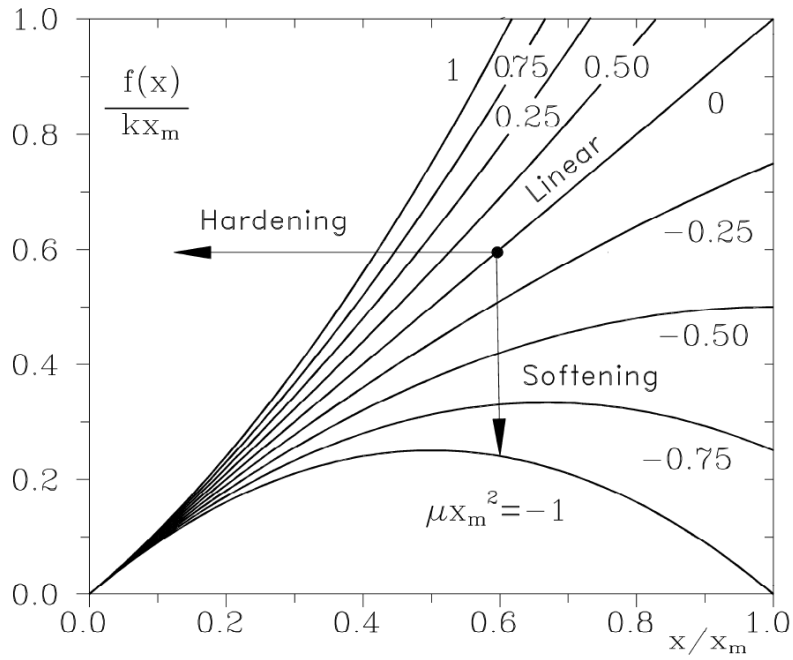


Figure 3.13. $f(x)$ at different μ [8]

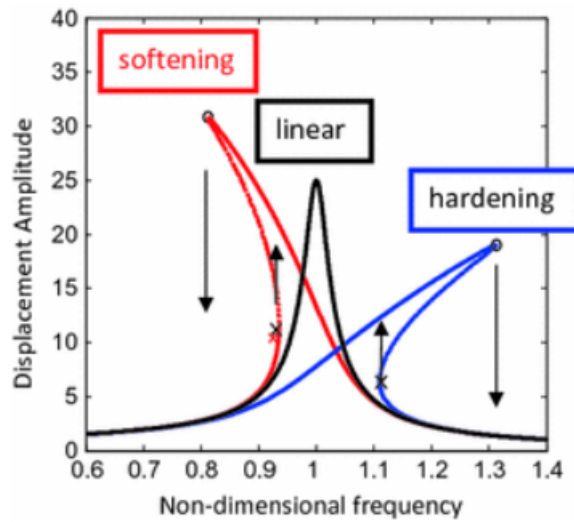


Figure 3.14. Non linear Displacement-frequency plot, comparison between hardening and softening behaviour [13]

Part II
Second Part

Chapter 4

Abaqus model

The model is the same described in sec. 3.1.2. For sake of clarity, below is reposed the studied system with load applied on its.



Figure 4.1. System with load

4.1 The problem of rigid body motion

The first thing to do is to compute the natural frequencies of the laminate, to do so it is used the step "Frequency" of Abaqus; it is important to do first of all this step because it is impossible to perform any type of linear perturbation analysis without it. After doing this the modes obtained are the three rigid body motion and the first 4 natural frequencies of the shell.

In order to check that all work well a first modal analysis, with a force of 10 N and a frequency equal to the first natural frequency of the shell applied in the middle of the bottom edge (fig 4.1), is taken out in an interval of 0.05 seconds with a sample time of 10^{-5} seconds; the step in Abaqus is called "Modal dynamics" and it refers to the data obtained by the "frequency" step to perform the computation. The displacement obtained in x_0 is plotted in fig 4.3.

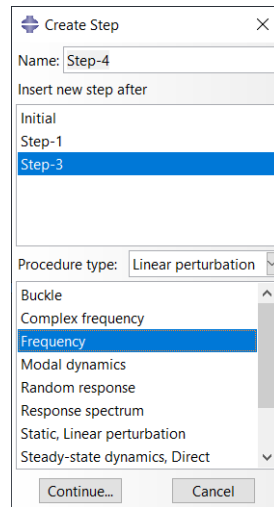


Figure 4.2. Linear perturbation steps

Nevertheless the result obtained is not so good, because of a translational motion of the shell associated to the expected mode 1 oscillation; it cannot be simply filtered because, when there will be taken into account the non linear components of the stiffness, the behaviour will probably completely change.

To face this drawback there are put 2 vertical constraints in correspondence of the nodal points of mode 1 (the points in which the vertical displacement at mode 1 is null). The resulting model is showed in fig. 4.4.

Obviously this last actions has to be tested, and so the following steps are followed.

1. In the "Frequency" step neglecting the rigid body motion
2. Performing the modal analysis ("*Modal dynamics*"), in a time of 0,05 s, of the non constrained model and collect the results
3. In the "Frequency" step consider even rigid body motions
4. Put vertical constraints in nodal points
5. Performing the modal analysis ("*Modal dynamics*"), in a time of 0,05 s, of the constrained model and collect the results

Without considering the rigid body motion and with a non constrained laminate, the result is a pure mode 1 behaviour of the laminate. while,

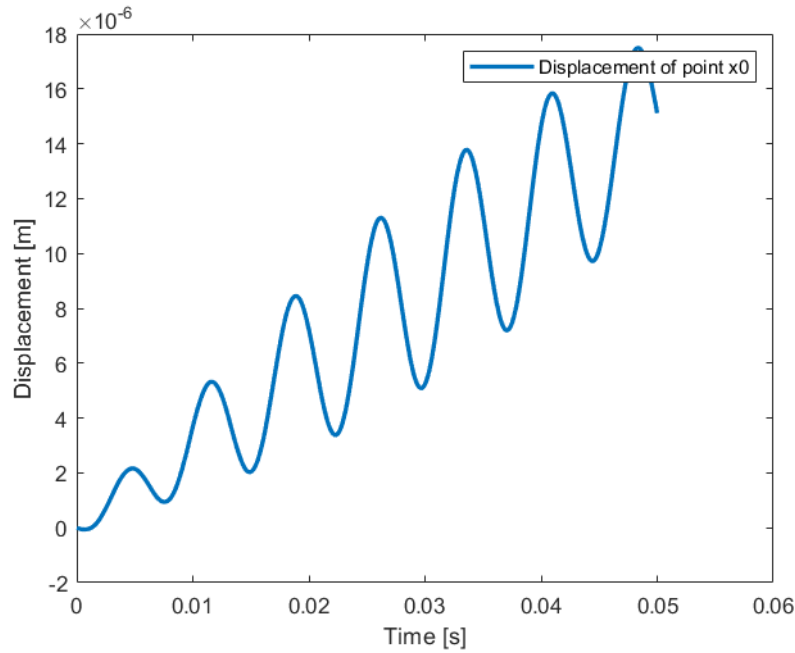
Figure 4.3. Displacement of x_0 

Figure 4.4. Model with pinned nodal points

when considering the rigid body motion in the "Linear perturbation step" and putting the constraints, the modal analysis and the integration in time give the same results. For this reason, from 2) to 4) both "Modal Analysis" and "Dynamic implicit" steps can be used; the first one has been chosen because requires less computation time.

4.1.1 Results

As it can be seen from the following plot, there are not significantly differences of stresses and displacements between the two cases; so it is possible to follow this way.

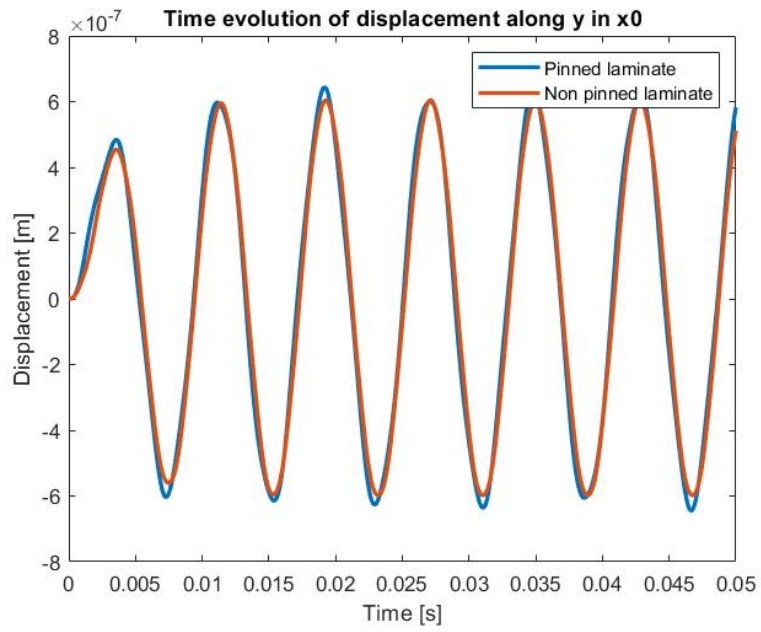


Figure 4.5. Displacement comparison

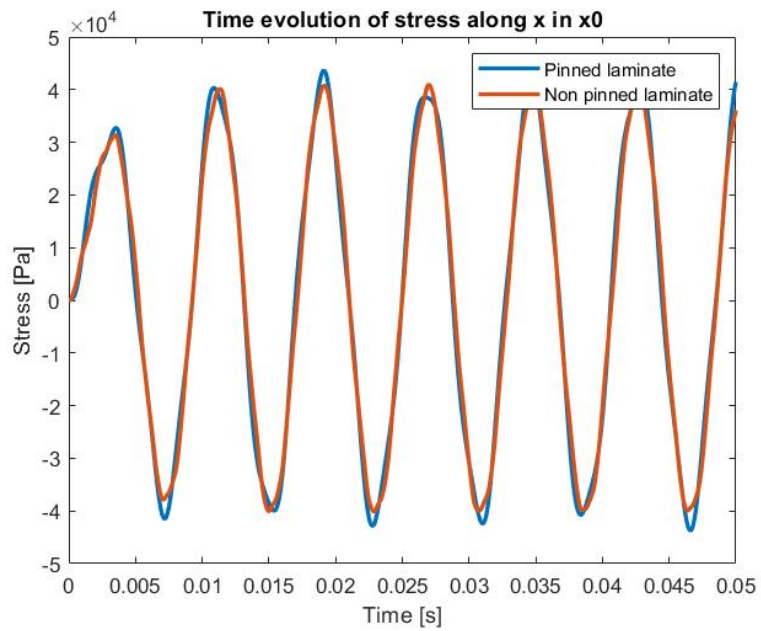


Figure 4.6. Stress comparison

4.2 Damping in Abaqus

In the dynamic implicit step of Abaqus it is not possible to define the damping of the material by simply inserting the damping ratio ζ ; in fact in the property of the material they are required α and β parameters of Rayleigh damping. The Rayleigh damping is expressed as a linear combination of both mass and stiffness matrix by the following formula [9]:

$$C = \alpha[M] + \beta[K] \quad (4.1)$$

Where:

[M] is the mass matrix

[K] is the stiffness matrix

it is not the scope of this dissertation to enter into the detail of how damping is computed, just in general the following equation is valid for the i^{th} natural frequency.

$$2\zeta_i\omega_i = \alpha + \beta\omega_i^2 \quad (4.2)$$

Where:

ζ_i is the critical damping ratio at mode i

ω_i is the i^{th} natural frequency

from the last one, considering the last equation, it is possible to obtain the following system [10]:

$$\begin{Bmatrix} \alpha \\ \beta \end{Bmatrix} = \frac{2\omega_i\omega_j}{\omega_j^2 - \omega_i^2} \begin{pmatrix} \omega_j & -\omega_i \\ -\frac{1}{\omega_j} & \frac{1}{\omega_i} \end{pmatrix} \begin{Bmatrix} \zeta_i \\ \zeta_j \end{Bmatrix} \quad (4.3)$$

if $\zeta_i = \zeta_j = \zeta$ the system can be simplified.

$$\begin{Bmatrix} \alpha \\ \beta \end{Bmatrix} = \frac{2\zeta}{\omega_i + \omega_j} \begin{Bmatrix} \omega_i\omega_j \\ 1 \end{Bmatrix} \quad (4.4)$$

Considering a damping ratio equal to 0.04 the following value of α and β are obtained.

Data	Value
α	46
β	$3 * 10^{-5}$

Table 4.1. Rayleigh parameters

4.3 Matlab automatization

As explained in sec. 3.2.2, there must be collected several values of displacement and nodal forces (along y and x) at every point involved in the crack growth; moreover the crack growth is simulated by removing in each simulation one attached node along the pre-specified pattern. Since all data have to be collected from a consistent number of simulation, a good code which can perform the job autonomously is required. To do so a preliminary system is created. The idea is to index all group of nodes attached, as can be seen in the following figures, and through Matlab at every simulation considering a different set of nodes. Obviously the nodes are enumerated in order to simulate the crack growing, so at the start all nodes are considered, apart from one which is the crack starting point.

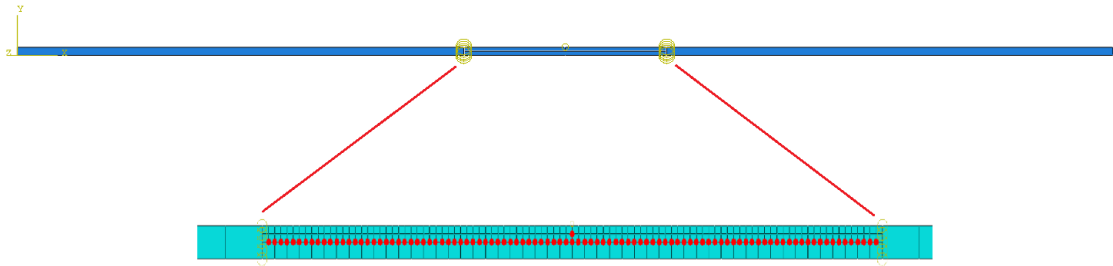


Figure 4.7. Zoom on the crack site, set of nodes "Node1"

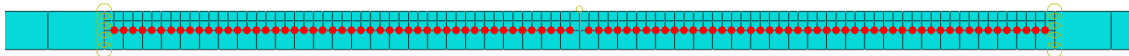


Figure 4.8. Zoom on the crack site, set of nodes "Node2"

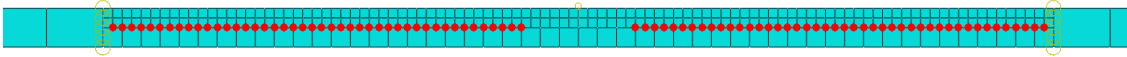


Figure 4.9. Zoom on the crack site, set of nodes "Node3"



Figure 4.10. Zoom on the crack site, set of nodes "Node4"

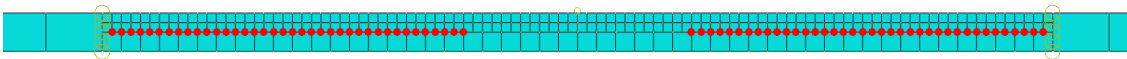


Figure 4.11. Zoom on the crack site, set of nodes "Node5"

Unfortunately the code created requires too much time to take the data from Abaqus, without counting the time that Abaqus takes to perform the simulation; for this reason it is abandoned. Nevertheless the code is proposed in chapter 6 because it took a lot of time to be written and it does what it is created to do, so it could be useful for future works.

4.4 Cohesive elements

It is considered the same model of sec. 4.3, at the edges evidenced in fig. 4.12 they are assigned the following interaction properties:

- **Tangential behaviour:** friction coefficient 0.05
- **Normal behaviour:** hard contact (linear case)
- **Cohesive behaviour:** only applied to the nodes considered



Figure 4.12. Edges considered in the interactions

It is important to point out that, in a first analysis, the node considered for the cohesive behaviour are the same evidenced in fig 4.8. The force is always applied in the middle of the bottom edge of the shell, at a frequency equal to the first natural frequency of the shell.

The last interaction properties are valid only for the linear case, in the non linear one the normal behaviour has to be changed, setting manually the stress-displacement curve (practically it is the stiffness behaviour). Considering the nodes at the mid point of the crack x_2 and x_3 (fig. 4.15), during the simulation they are separated and the displacement are reported in fig 4.16; it is proposed a zoom at one of the peak of the two curves because they are very near each other.

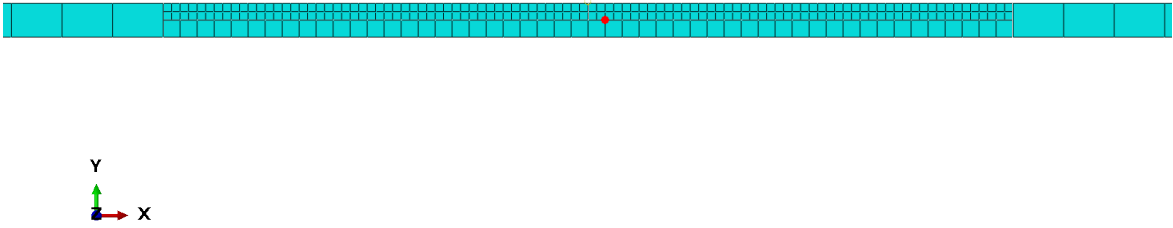


Figure 4.13. Point considered to take data x_1

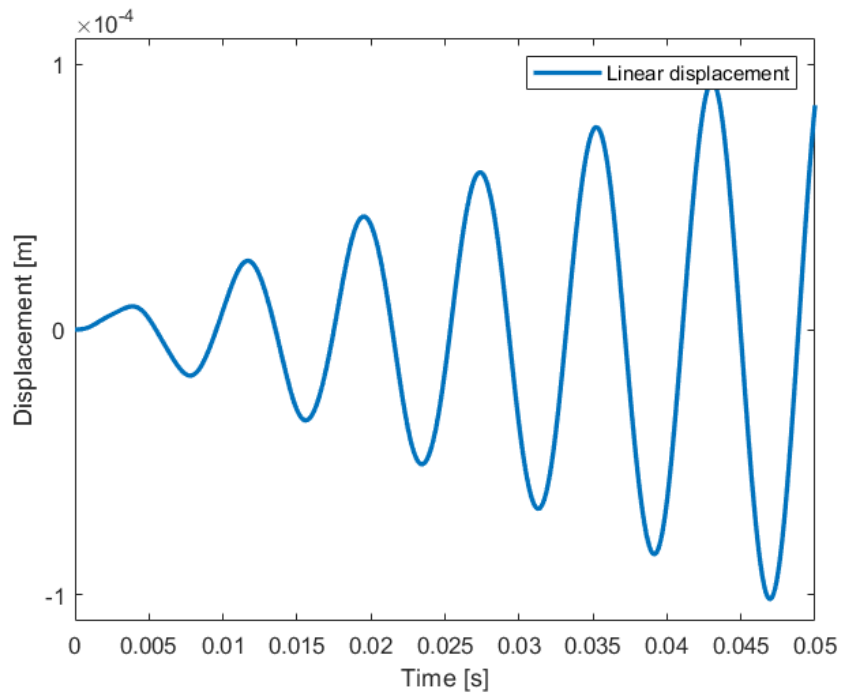


Figure 4.14. Displacement of point x_1 in linear case

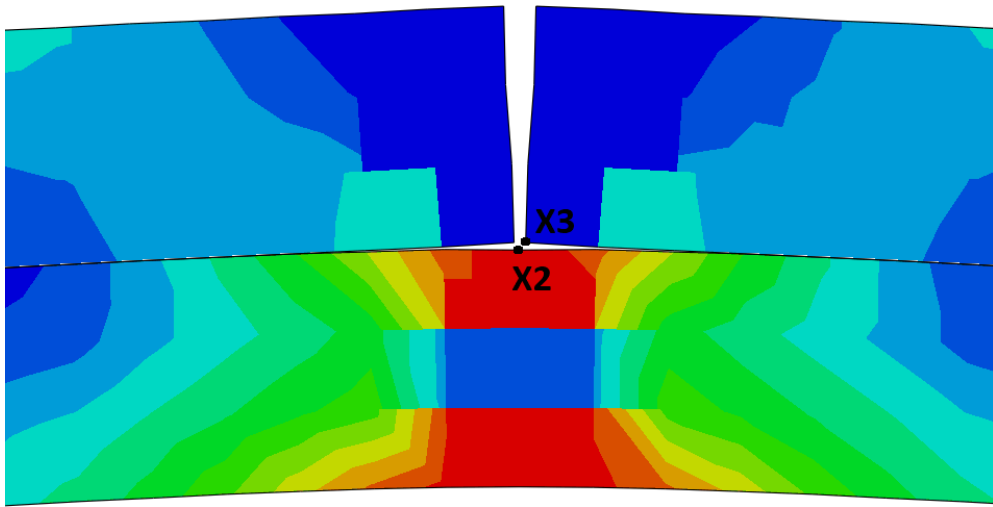


Figure 4.15. Deformation at crack initialization

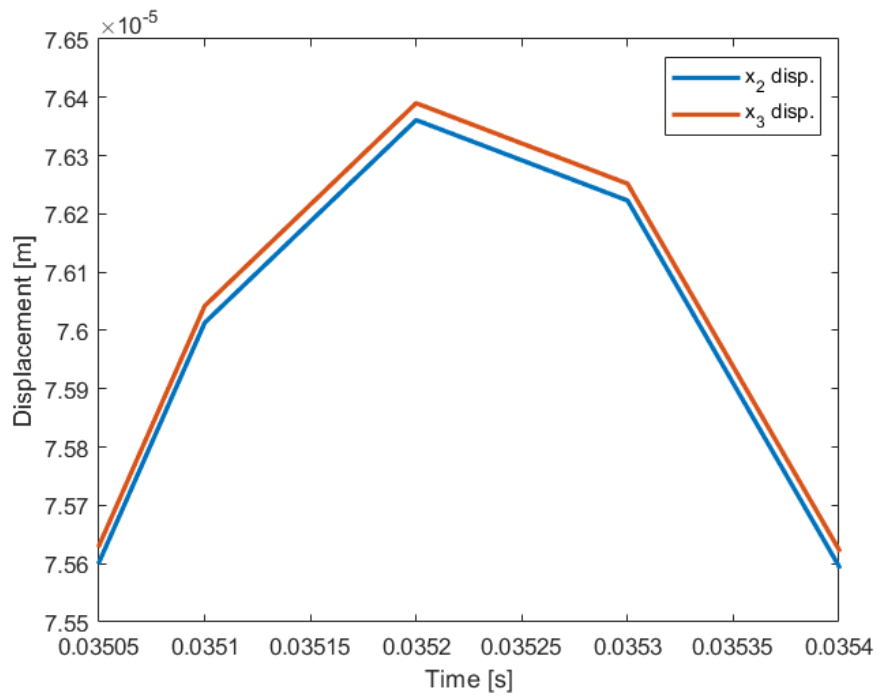


Figure 4.16. Displacement of point x_3 and x_2

Based on the curve of fig 4.16 it is chosen the following type of stress-displacement curve, by considering the stiffness linear until $2 * 10^{-9}m$ with value equal to the stiffness of the material ($210 * 10^9 MPa$), and a cubic behaviour from that on.

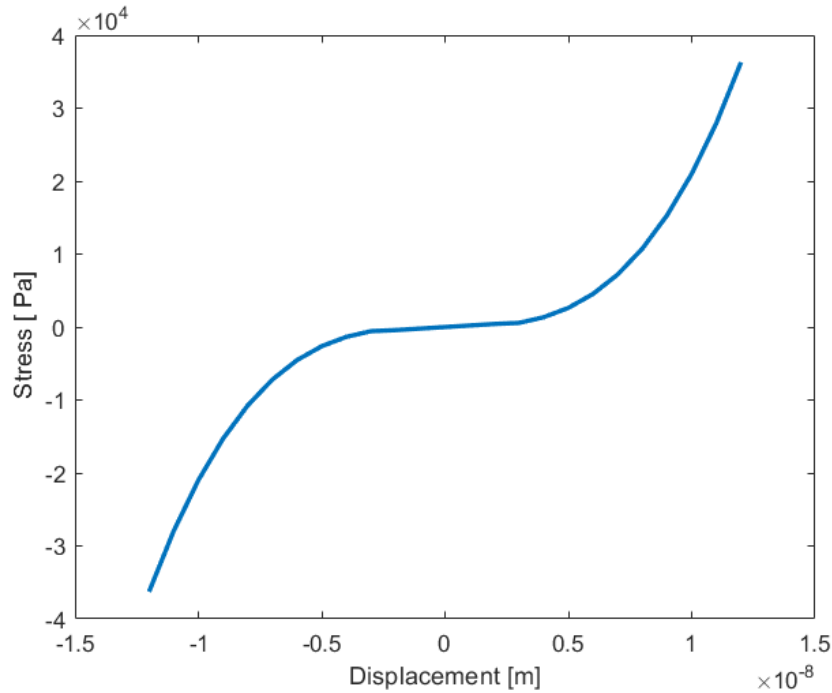


Figure 4.17. Non linear stiffness

Performing the analysis in both linear and non linear case, as expected, the absolute value of the resulting displacement curve in point x_1 is slightly lower in the second case (fig. 4.18), this is due to the hardening phenomena discussed in sec. 3.3.1.

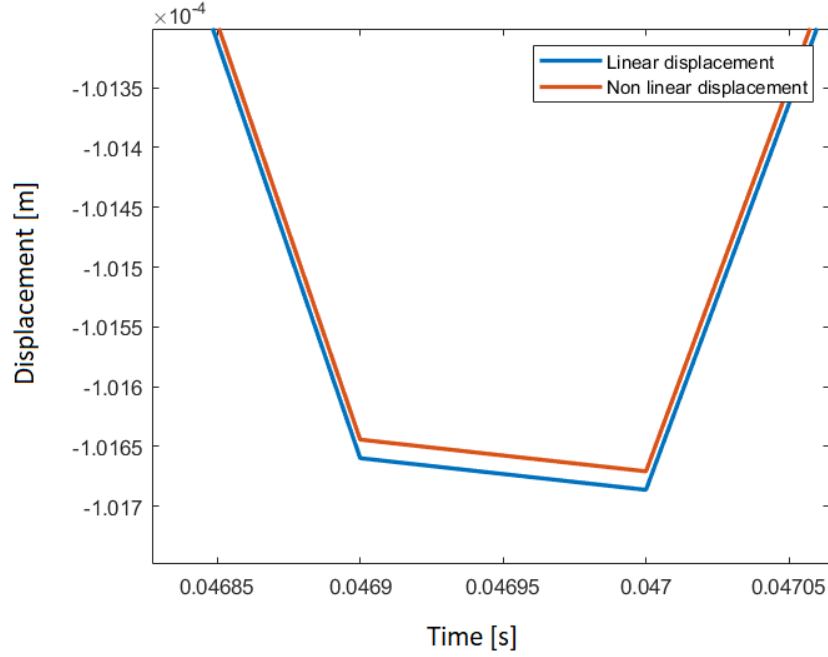


Figure 4.18. Displacement of point x_1

Considering the stress component along y (fig. 4.20) at the point x_1 it appears a problem; there are some frequency components too high (fig. 4.19) which make the results incompatible with the scope of the research. The reason of this drawback is associated to the cohesive behaviour, the message file of Abaqus reports several warnings during the simulation, but it is not well clear why. For this reason even the cohesive behaviour is put aside.

Nevertheless it is kind of interesting to give a look at the stress behaviour. In fact, despite the bad results, it is possible to individuate a significant trend. The stress in the non linear case is always higher than the stress in the linear one, as can be seen by fig. 4.21; this is another time due to the hardening phenomena. Then another problem appears from this plot, in fact the stress component, which is expected to be of the same amplitude in both tension and compression, appears much more high in the last case. In detail the problem is due to the fact that, in the cohesive behaviour, Abaqus consider the non linear behaviour only when the overclosure is positive, which practically means that the laminate acts as a non linear material only in compression; this last discovery make completely useless the cohesive interaction for the scope of this thesis, because the VCCT is mainly focused on the tension behaviour.

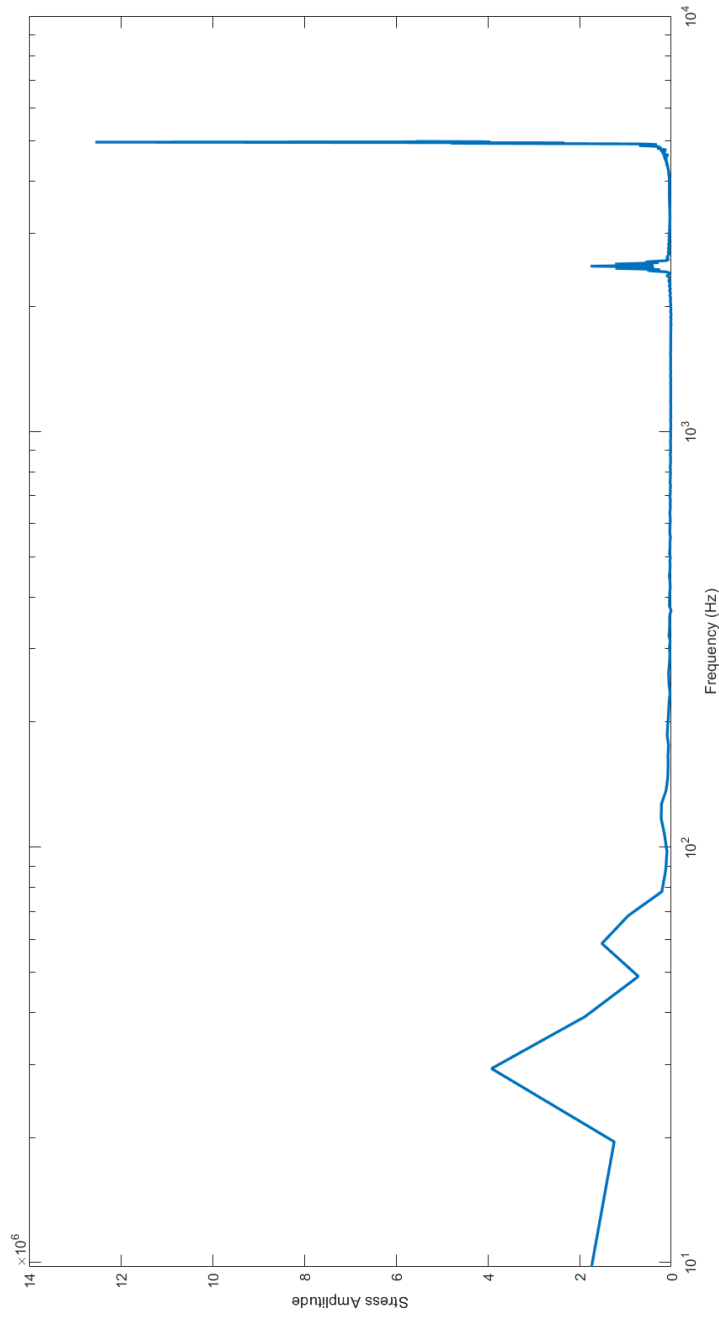


Figure 4.19. Fast Fourier transform of linear stress in x_1

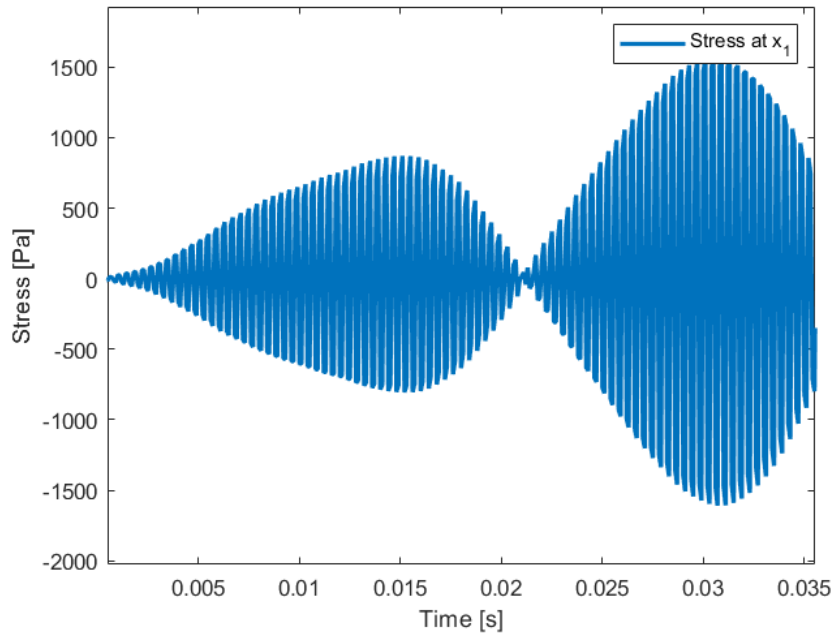


Figure 4.20. Vertical stress at point x_1

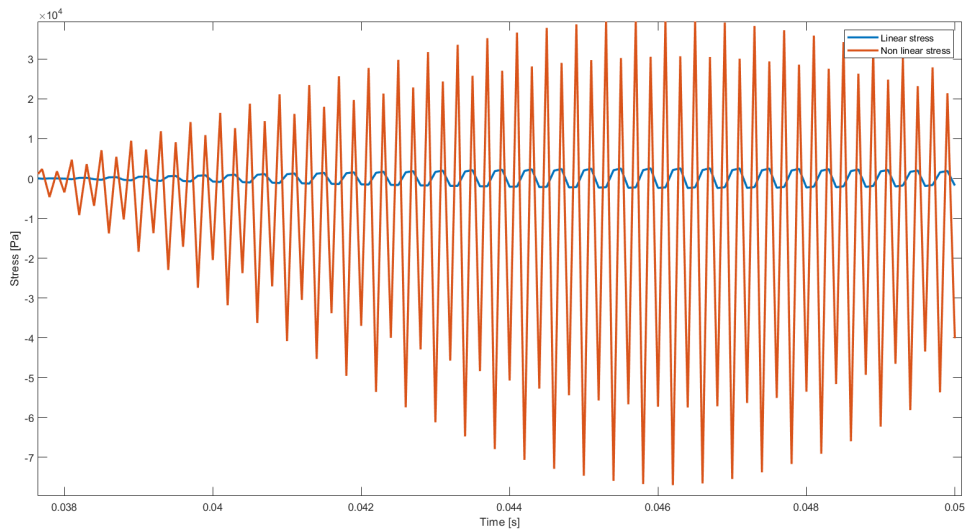


Figure 4.21. Vertical stress at point x_1 in both linear and non linear case

4.5 Final model (Case 1)

At this point it is chosen another way to face the experience; since the cohesive interaction is revealed not suitable to the studied case, the idea is to put some springs between the nodes involved in the crack propagation (remembering that the path of the crack growth is pre specified). The path is changed, in order to make more significant the buckling phenomena which will affect the response of the system to external excitations. In fig. 4.22 is represented the new system in which the delamination does no more cut the laminate in the middle, rather the crack develops near the top surface.

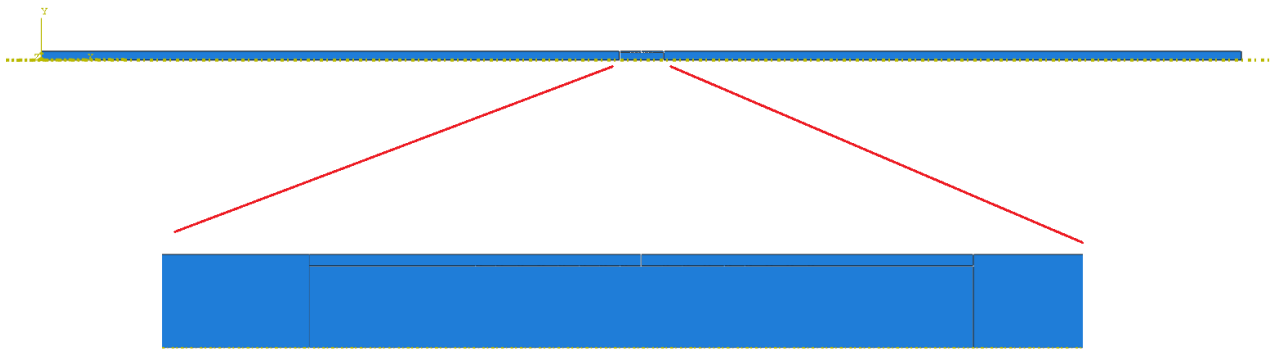


Figure 4.22. New crack path

From now on the interest is only on the delamination phenomena, neglecting the vertical evolution of the crack; so at the starting point the nodes in the vertical edge of the crack are not connected (but it is still present the normal behaviour of the contact properties in order to avoid the interference), while in the horizontal edge there are 16 springs in total (fig. 4.23).

At this point the problem is to correctly determinate the stiffness of the spring. This is needed because the spring acts along a line and not on a surface, for this reason it is not possible to use the young modulus in this simulation. It is practically done by comparing the displacement at one of the node involved in the delamination in both the following case:

- non cracked laminate
- laminate with springs

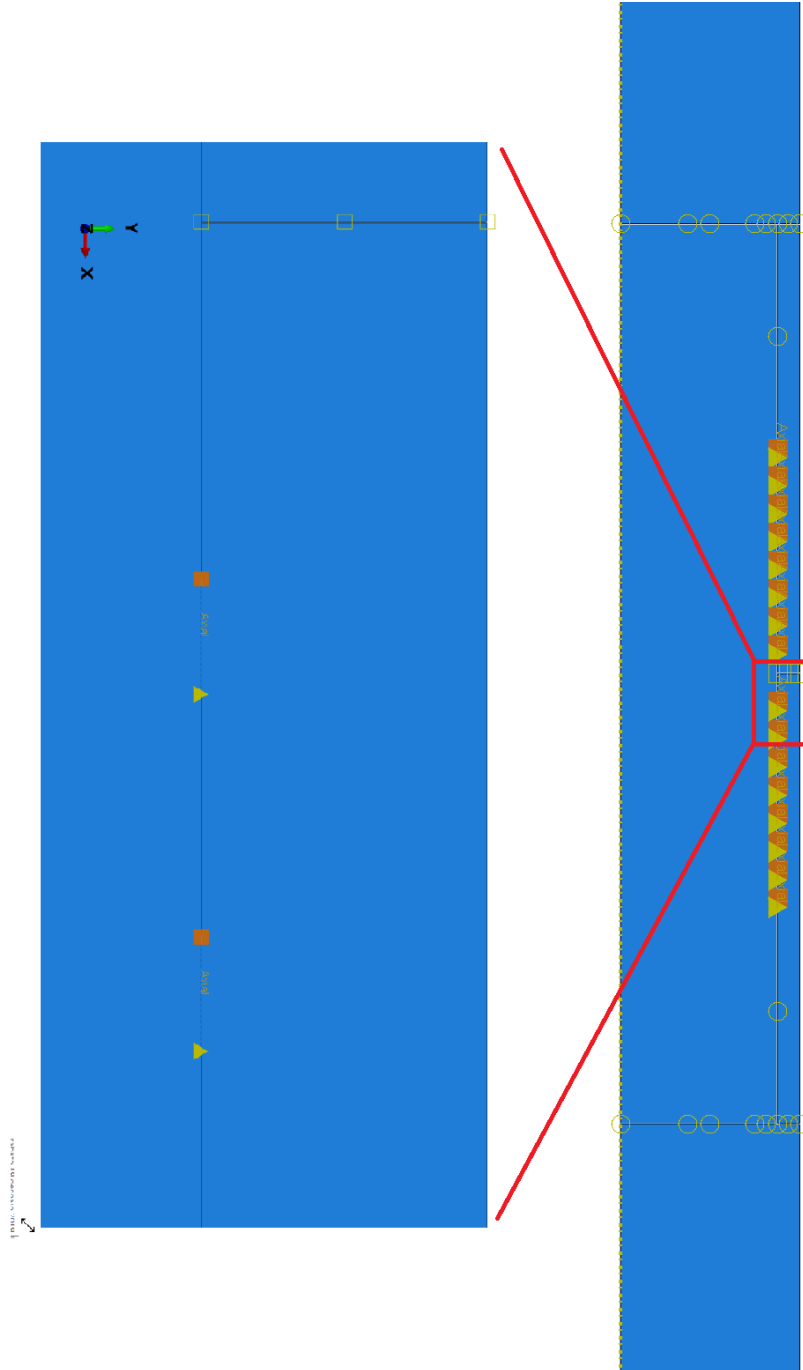


Figure 4.23. Zoom on the springs on the crack path

The comparison is repeated, changing the stiffness value every time, until the displacement curve fit enough to be considered valid. In the end the stiffness value chosen is the following:

$$K = 1,5 * 10^{10} N/m \quad (4.5)$$

At this point it is done the same procedure done in the last section, and so the non linear stiffness curve is obtained by considering the linearity only in the range between 0 and $2 * 10^{-8}$ m.

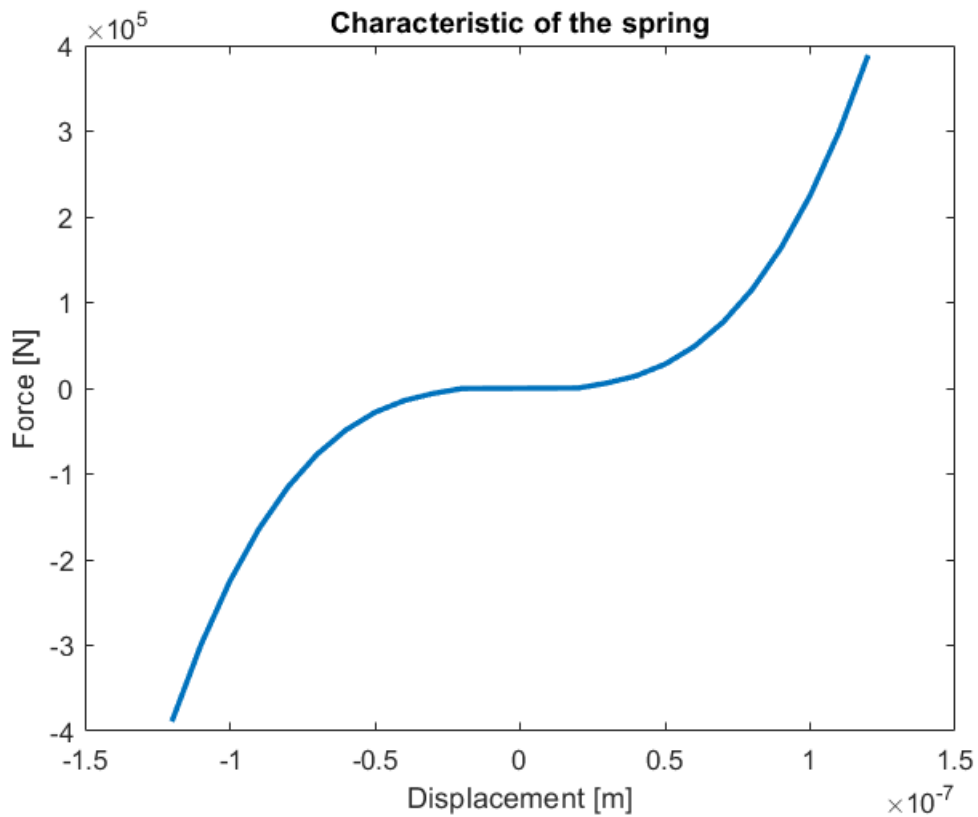


Figure 4.24. Non linear spring characteristic

4.5.1 Procedure for crack growth evaluation

In order to evaluate the crack growth in time along the x direction the following iter has to be followed.

1. In the spring properties selecting the linear behaviour of the springs.
2. Performing the simulation.
3. Taking the value of vertical displacement in time for x_2 and x_3 (fig. 4.25).

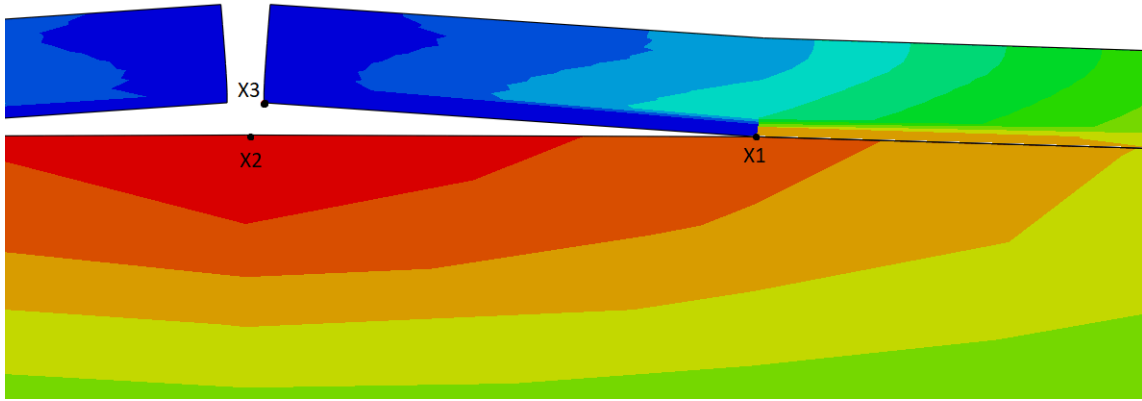


Figure 4.25. Zoom on the crack

4. taking the value of vertical force in time at point x_1 .
5. Considering the maximum absolute value of Force F_y from fig. 4.27.
6. Considering the maximum absolute value of the difference between the displacement of point x_2 and point x_3 Δw from fig. 4.28.
7. Regarding the Paris' law parameters, since the purpose of this thesis is to qualitatively compare two cases which are both analysed by the software, they can be assumed arbitrarily because they are valid for both linear and non linear case. Russell and Street [12] find another shape of the Paris' law, which connect the crack growth rate with the strain energy release rate (SERR) instead of the stress strain rate; it is much more suitable for this case because from VCCT it is obtained directly the SERR.

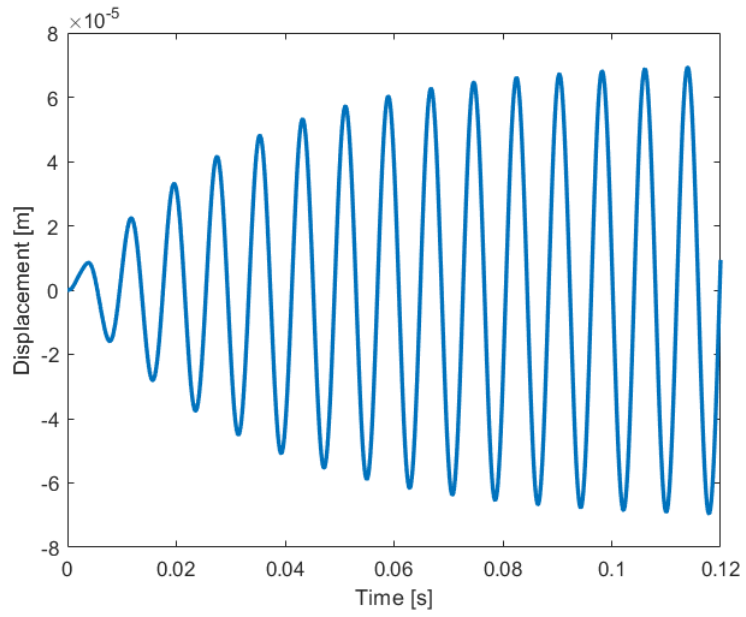


Figure 4.26. Displacement in time at point x_2

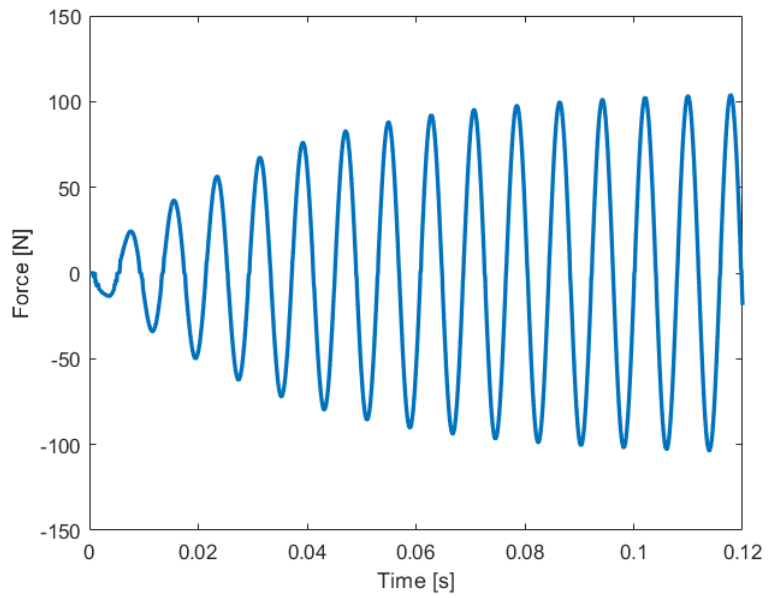


Figure 4.27. Force in time at point x_1

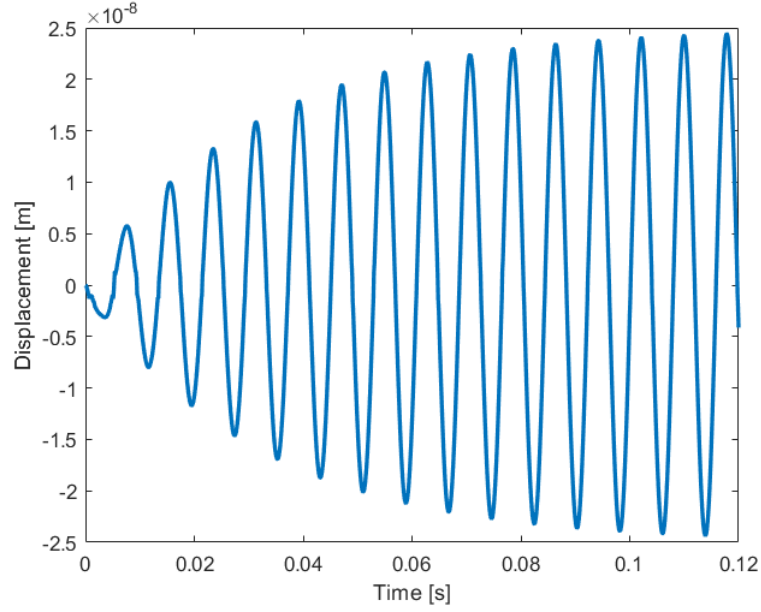


Figure 4.28. Difference between the displacement of point x_2 and point x_3

$$\frac{da}{dN} = C \left(\frac{\Delta G}{G_c} \right)^m \quad (4.6)$$

Where:

ΔG is the difference between maximum and minimum SERR.

G_c is the critical SERR obtained by the fracture toughness (Eq. 4.8) of the material.

From literature they are find the following value of the parameters for a steel laminate of similar geometry.

$$C = 5,6 * 10^{-8} \frac{m}{\text{Cycle} * \text{MPa} * \sqrt{m}} \quad (4.7)$$

$$K_c = 50 \text{MPa} \sqrt{m} \quad (4.8)$$

$$m = 3,25 \quad (4.9)$$

and so:

$$G_c = \frac{K_c^2}{E} = \frac{50^2}{210 * 10^3} MPa m = 0,0119 MPa m \quad (4.10)$$

8. They have to be obtained the values of maximum strain energy release rate by using the equation 3.18, here reported with the variables' name changed for sake of clarity.

$$G_I = -\frac{1}{2\Delta a} F_y \Delta w \quad (4.11)$$

Since the stress ratio is $R=-1$, as can be seen by fig 4.29, the absolute value of $G_{I_{max}}$ and $G_{I_{min}}$ are the same, so when applying the Paris law it becomes:

$$\frac{da}{dN} = C \left(\frac{\Delta G_I}{G_{Ic}} \right)^m = C \left(\frac{2G_{I_{max}}}{G_{Ic}} \right)^m \quad (4.12)$$

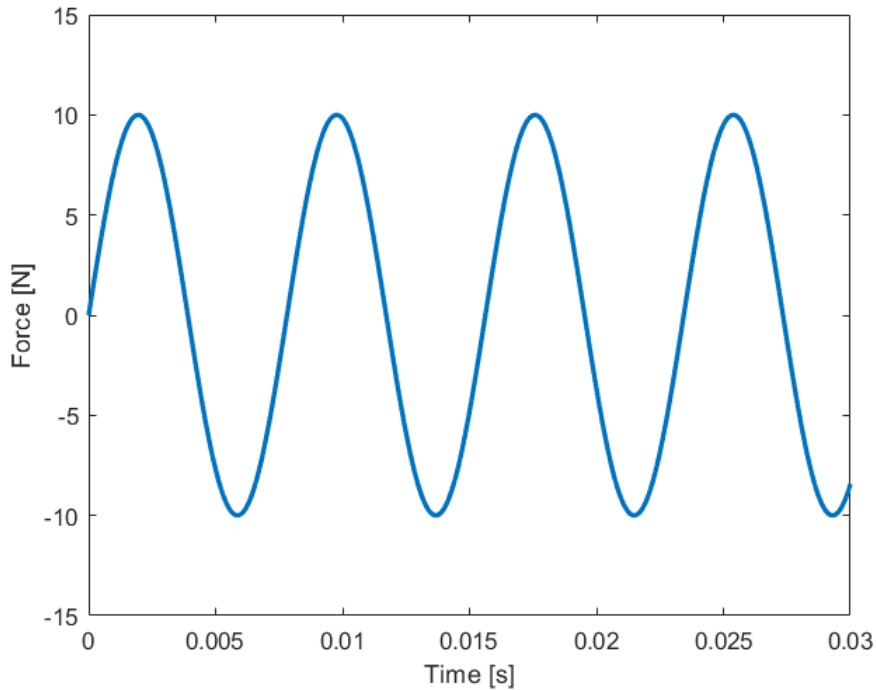


Figure 4.29. External load in time

9. The edge of the single mesh element chosen is $\Delta a = 3.125 * 10^{-4}$ and so, once computed the value of G_I , it is possible to enter into the discrete Paris' law equation, obtaining the number of cycle needed to make the crack open along Δa

$$N_{n+1} = N_n + \frac{\Delta a}{C \left[\frac{2G_{I_{max}}}{G_{Ic}} \right]^m} \quad (n = 0, 1, \dots, N) \quad (4.13)$$

10. At this point saving the data and:

- if the simulation performed was linear, repeat all passages from 1) but selecting the non linear behaviour of the spring.
- If the simulation performed was non linear, eliminate the spring at the last connected part and repeat all passages from 1)

4.5.2 Results

In this section they are collected all the main results. For example in fig. 4.30 it is shown the crack growth behaviour comparison between linear and non linear stiffness.

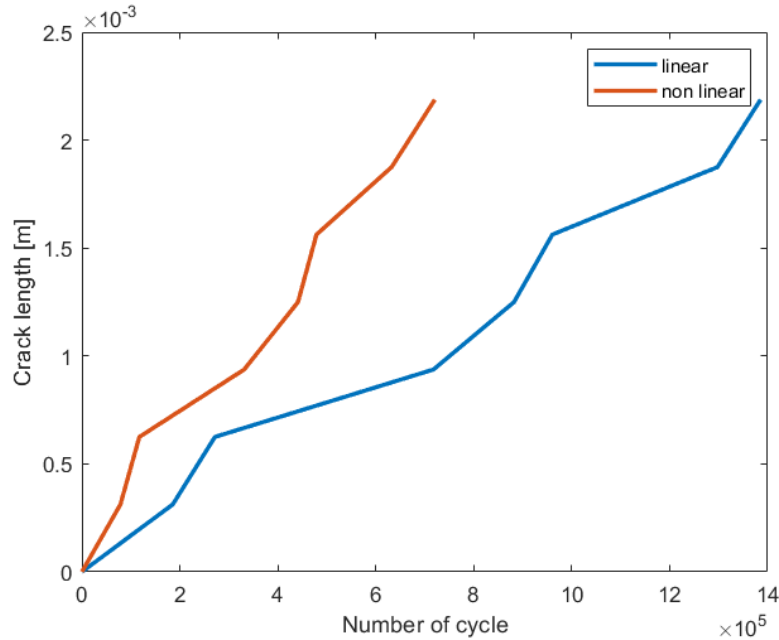


Figure 4.30. Crack growth rate comparison

It appears quite clear that the non linear stiffness make the crack open much more rapidly than the linear case, it is interesting because it suggest that there is a big difference in the life of the material by considering the cubic field of stiffness. Nevertheless this result is not a surprise, it was expected a lower life in the non linear case because stresses at the same displacement are higher than those obtained in the linear one; but the difference was supposed to be not so important, while for the cubic behaviour of stiffness chosen the life is practically halved.

It should be even interesting to look at the frequency content of the force in the last contact point of every step (for example the node x_1 in fig. 4.25); practically they are taken all the values of F_y in time and they are compared in order to figure out which harmonics are excited and how the amplitude of every harmonic change.

First of all it is needed a comparison between the linear case and non linear one of the first step, so the case in fig. 4.25.

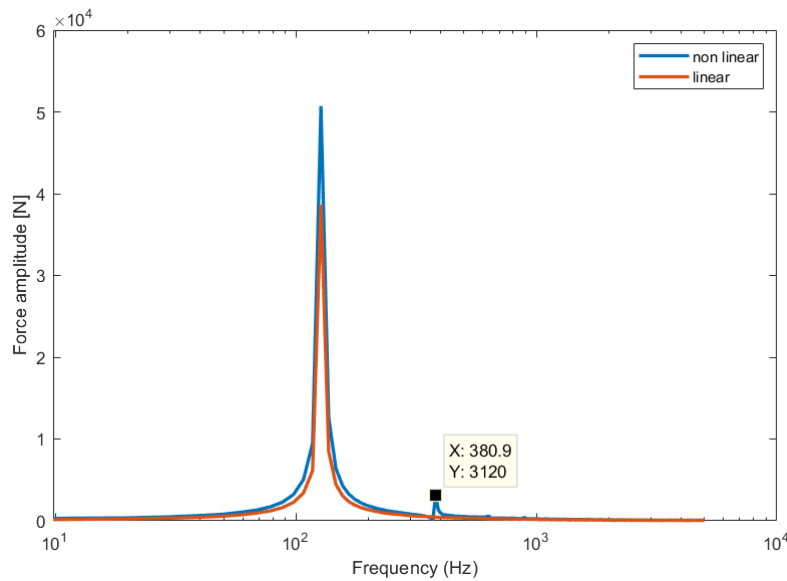


Figure 4.31. Comparison between FFT of the linear and non linear case

From the last figure it is firstly possible to see that, at the first natural frequency, the magnitude of the force is higher for the non linear stiffness case, something that has been discussed before, but another confirm of the hardening behaviour. Focusing at higher frequency there are some peaks in the non linear curve which are not present in the linear one; this was predicted in sec. 3.3.1.

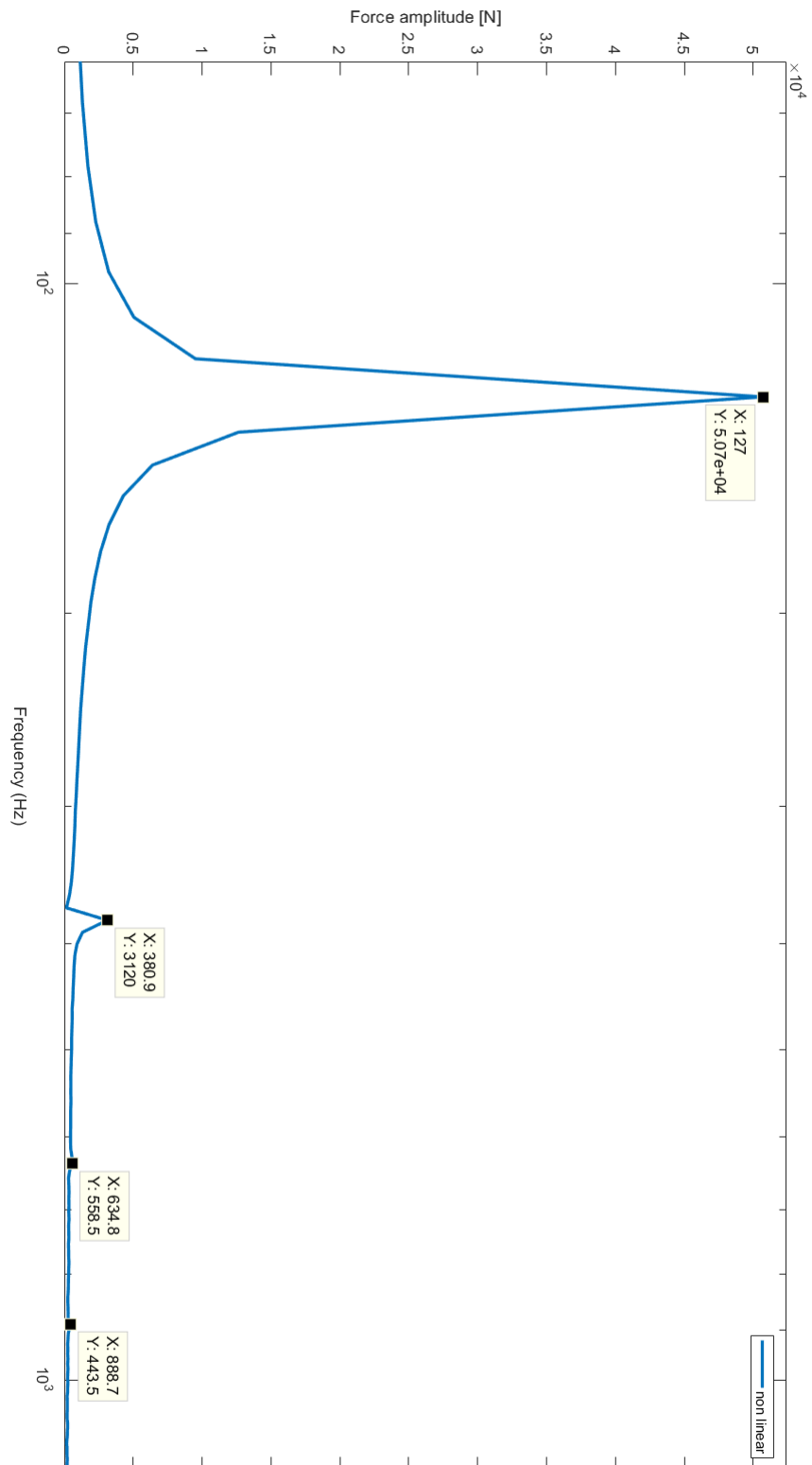


Figure 4.32. FFT of non linear case

In fact a better look shows that the peaks appears only at odd multiple of the first natural frequency, it can be better appreciated in fig. 4.32. The point evidenced in fig 4.32 correspond to the third, fifth and seventh multiple of 127 Hz. Since the amplitude of the first harmonic is too large to be compared with the others, a magnification of the last three multiple is occurred.

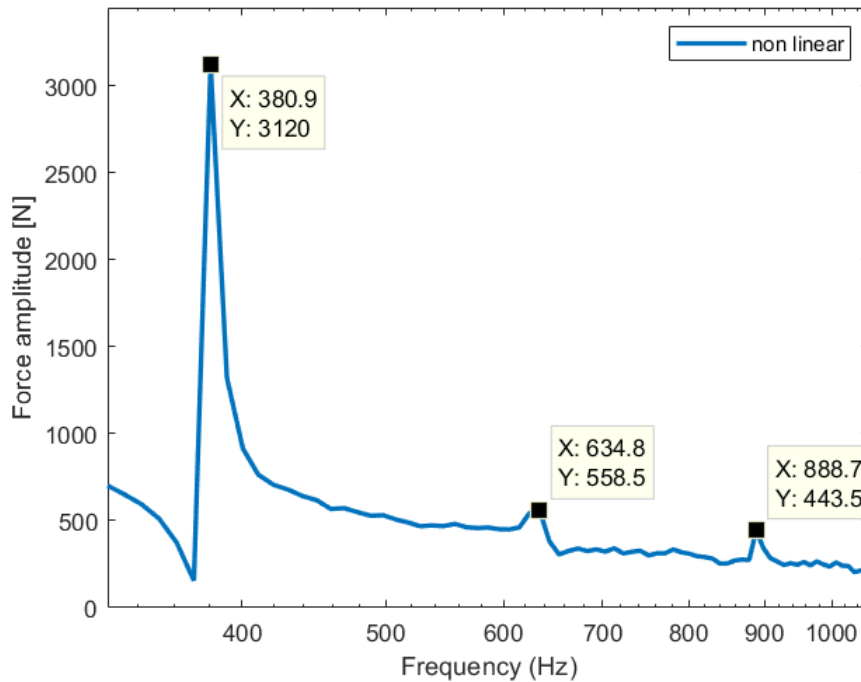


Figure 4.33. Third, fifth and seventh multiple of the main harmonic

Let focus on the amplitude of first harmonic, it changes during the crack propagation, as can be seen in fig. 4.34; the number of the curve indicate the crack propagation step, remembering that the single step is long $3,125 * 10^{-4}m$.

In order to make the results much more clear, it is worth to consider the amplitude of the first and third harmonic in a plot which compare directly them with the crack propagation.

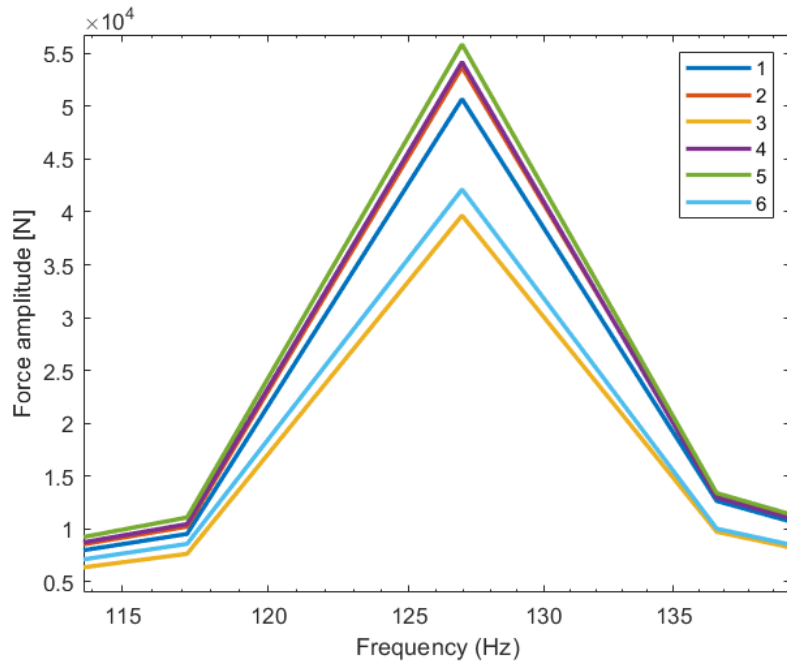


Figure 4.34. First harmonic during crack propagation

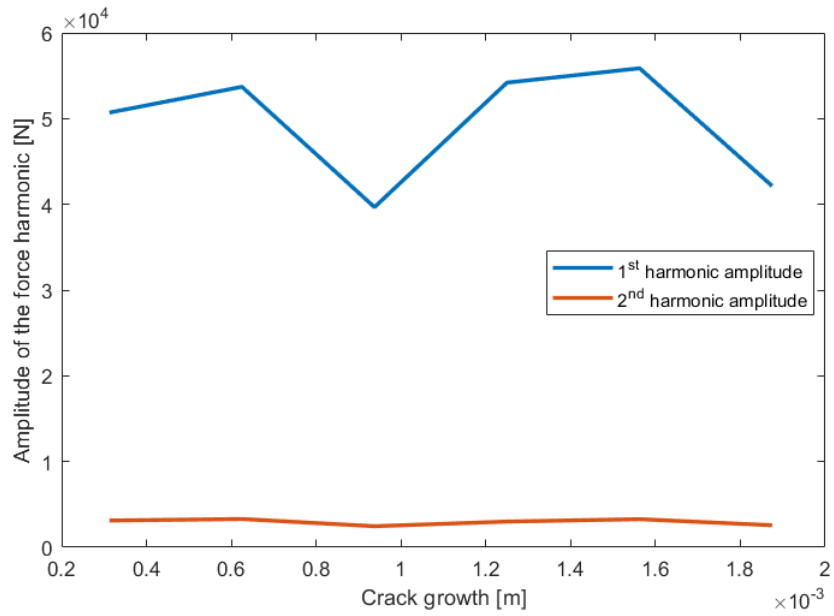


Figure 4.35. First and third harmonic during crack propagation

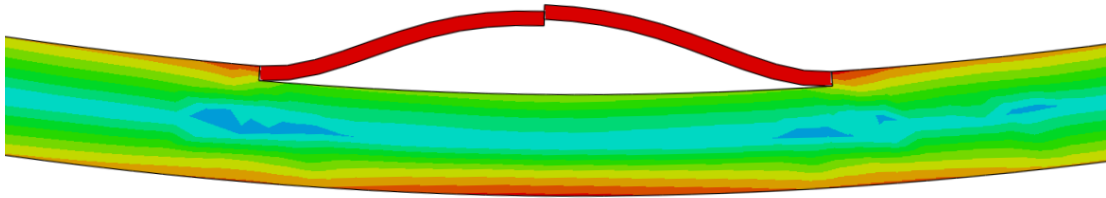


Figure 4.36. Buckling in compression

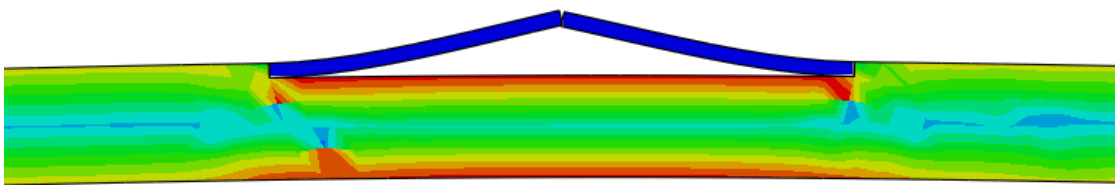


Figure 4.37. Tensional behaviour

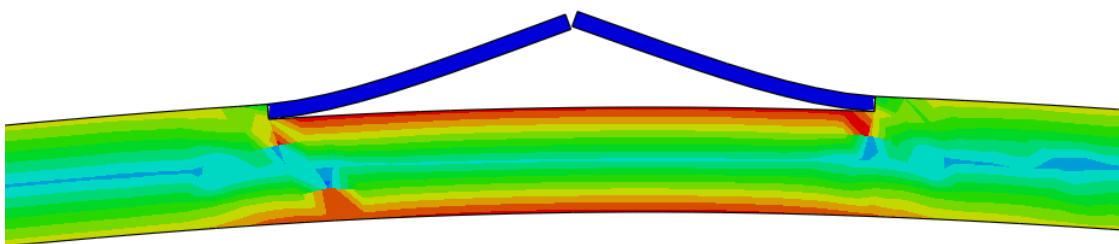


Figure 4.38. Tensional behaviour without contact

There are some significant drop in the amplitude of the first harmonic, giving a better look to the simulation it appears a phenomena which seems explaining this behaviour. In fact the buckling phenomena could cause a lower displacement in the tension phase, it can be figured out by fig. 4.37 and 4.38. In fact in fig. 4.38 they are not present the contact properties between the vertical crack surfaces and this shown that at every node of the crack the vertical displacement is considerably higher than the case with contact; so more the crack is open, more this phenomena take place and so, since the distance between the surfaces is smaller than the case without buckling, in turn the resulting force is smaller.

4.6 Final model (Case 2)

It could be worth to perform the same analysis of the last section on the model with the crack opened in the middle (fig.4.40)

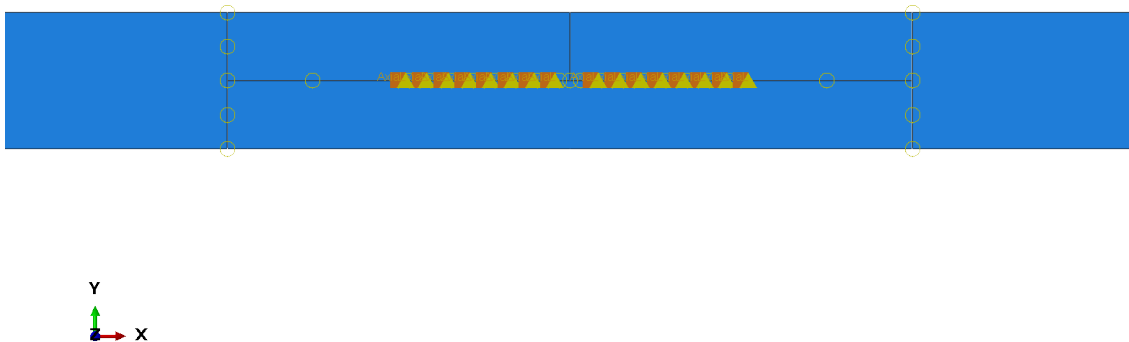


Figure 4.39. Model with springs

The number of springs and the operative procedure between the two case are the same. So the crack growth is represented by using the same parameter of the case 1, for both linear and non linear springs.

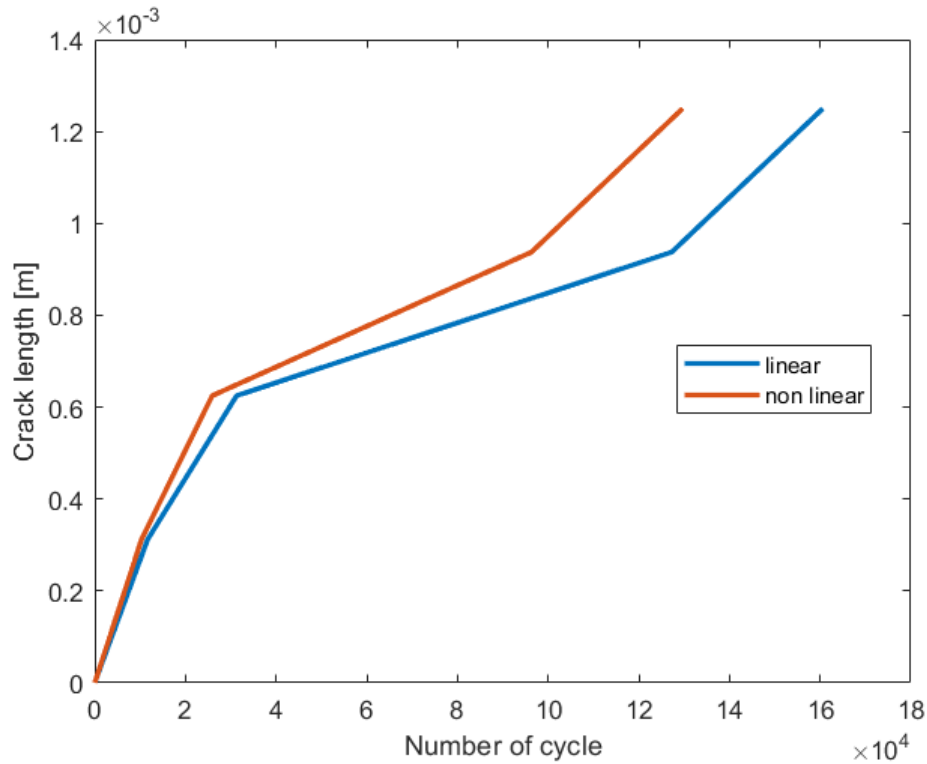


Figure 4.40. Crack growth rate comparison (case 2)

It appears clear that the behaviour in this case is practically the same of the other one, but the non linearity effects are not so evident; in fact, while in the case 1 the life with non linear effects was practically halved, in this case the reduction is only about the 25%.

By plotting the Fast Fourier Transform of the force at the last connected spring it appears something different respect the case 1: all the multiple, both even and odd, of the forcing frequency are excited, furthermore the odd harmonics appears to be lower in amplitude than the even ones.

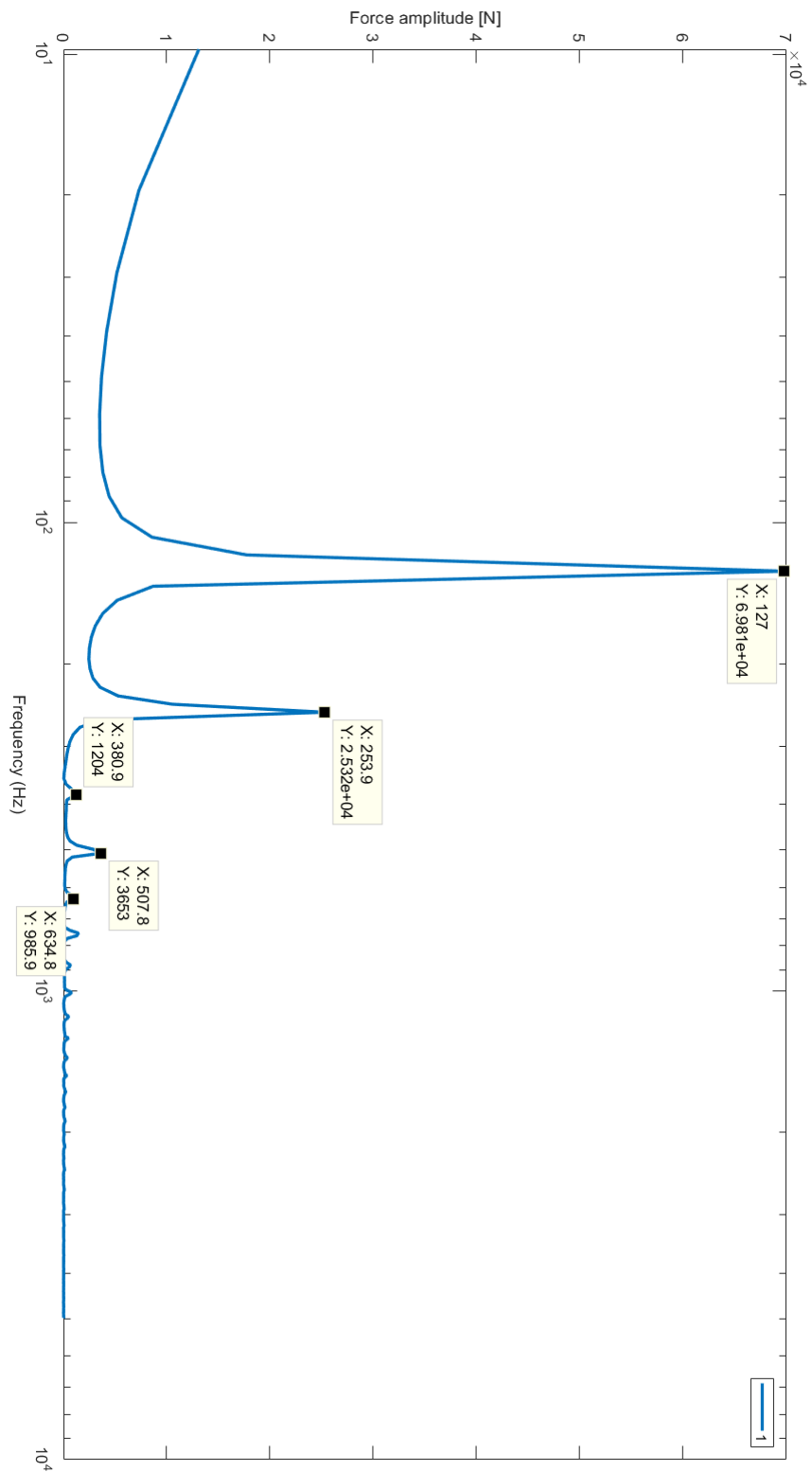


Figure 4.41. Fast Fourier Transform of the force with non linear spring (case 2)

The first harmonic amplitude changes in the way showed in fig.4.42, even in this case there are some peaks and some drops which could be explained with the buckling phenomena.

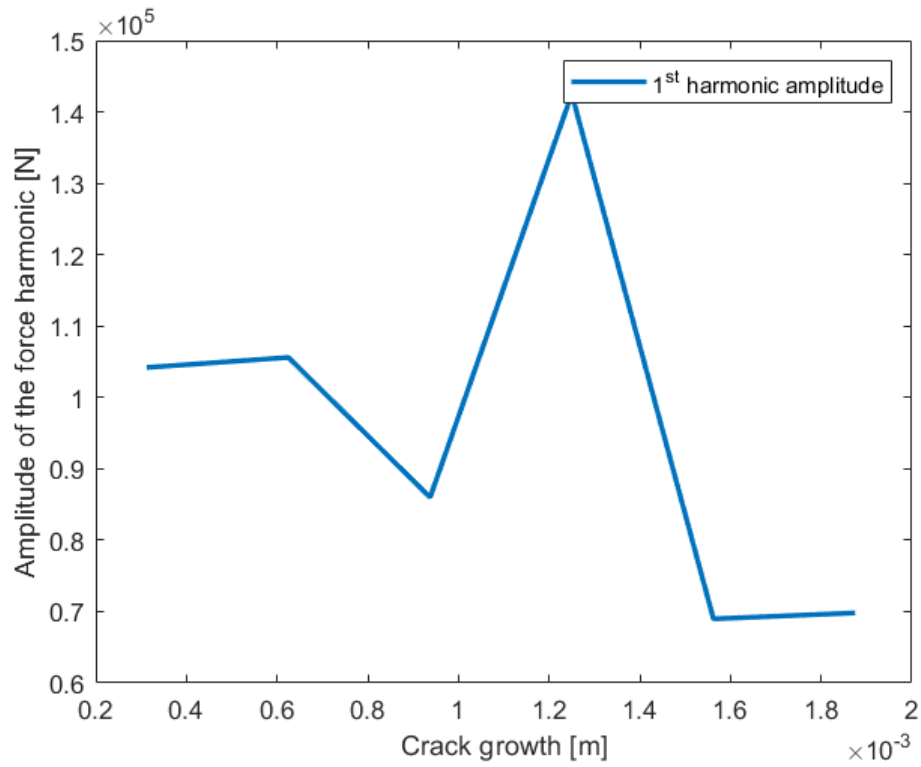


Figure 4.42. Crack growth rate comparison (case 2)

Chapter 5

Conclusions

The aim of this thesis, titled "Stiffness reduction caused by vibration fatigue", was to perform the following objective:

- understanding how delamination behaves in a laminate;
- create a suitable model in Abaqus;
- compare the linear model with the non linear one.

In chapter 3.2 is showed for the first time the technique which will be used in the second part of the thesis to compute the crack growth rate, the "Virtual crack closure technique". Thanks to this method, associated to the Paris'law, it is possible to predict the failure of the specimen by taking several values of displacement and force after the simulation by FEM software, in this case Abaqus.

By performing the simulation at cyclic bending load, it appeared a problem connected to the rigid body motions of the laminate; for this reason, in chapter 4.1, a solution to this problem is provided by constraining the nodal point at first mode of vibration of the laminate.

Once the model is well defined, and the operative procedure was established, in order to perform all the simulation needed an automatization was required (as explained in chapter 4.3). Unfortunately this way has not been pursued because of the large time of computation required.

In the end, after several attempts, the choice to connect the surface on the crack path with springs appears to be the unique suitable to the purpose of this thesis. The results obtained are interesting because suggests that non linearities in a material can highly decrease the life of the component, a result far then what supposed, at least in the amount of decreasing. It is

fairly worth the analysis of the FFT showed in sec. 4.5.2, because it appears something strange at certain crack length; after several checks it is found out a phenomena which appears at crack level and make the force acting on the springs lower than what expected: the buckling phenomena. A deeper explanation of this phenomena is forward the scope of this thesis, the main objective was to demonstrate how the life of the laminate changes with non linearities, and from the two cases analysed it can be assessed without any doubts that it decreases. The amount of the decrease depends on many factors, for example the fatigue parameter chosen, or as seen in the last chapter the depth of the delamination. In fact higher is the depth, much more the non linearity effects on the component life appears to be smoother.

5.1 Future work

In this thesis all the simulation are performed with fixed properties of the material; nevertheless it could be worth to consider the local friction at crack site, which makes the temperature of the material increasing and so its properties change in turn. For this reason the failure behaviour should be modified and results could be much more different from what studied here. Obviously they are required many more data from experiment, in order to predict how the properties depend by temperature, and in this way modifying them at each step of the simulation.

Chapter 6

Matlab code

```
clear all ;close all ;clc

%%
Py_file='delamination';

for k=1:1

    %% Defining files

    if k==1
        fid = fopen([Py_file,num2str(k-1),'.py'],'rt') ;
        X = fread(fid) ;
        fclose(fid) ;
        X1 = char(X.' ) ;
        IND = strfind(X1,'rootAssembly.sets[');
        for j=2:3
            X=[X(1:IND(j)+23);num2str(k);X(IND(j)+25:end)];
            X1 = char(X.' ) ;
            fid2 = fopen([Py_file,num2str(k),'.py'],'wt') ;
            fwrite(fid2,X1) ;
            fclose (fid2) ;
        end
        if k==2
            IND1 = strfind(X1,'thickness=0N');
            fid = fopen(['Int3.txt'],'rt') ;
            String= fread(fid) ;
            fclose(fid) ;

            X=[X(1:IND1(end)+14);10;String;X(IND1(end)+16:end)];
            X1 = char(X.' ) ;

            fid2 = fopen([Py_file,num2str(k),'.py'],'wt') ;
            fwrite(fid2,X1) ;
            fclose (fid2) ;
        end
    end

    abd='script';
```

```

endtime=1
Dat_file_end='delamination';
Pari='pari'; %it is used to set the end of abaqus running
%%

system(['abaqus cae ',abd,'=',Py_file,num2str(k),'.py & ']); %la & serve a non farlo andare in
loop

sw=true;
while sw
    % Pause Matlab execution in order for the lck file to be created
    pause(0.5);
    % While the lck file exists, pause Matlab execution. If it is
    % deleted, exit the while loop and proceed.
    while exist([Pari,'.txt'],'file')==2
        pause(0.1)
        % the log file has been created and Matlab halts in this loop.
        % Set sw to false to break the outer while loop and continue
        % the code execution.
        sw=false;
        break %it is necessary because the second while is a loop
    end
end
delete('pari.txt')
%% modifying the .inp file

fid = fopen([Dat_file_end,'.inp'],'rt') ;
X = fread(fid) ;
fclose(fid) ;

S1='D:\temp\delamination 2\A2M_GUI_Output'
cd(S1) ;

X1 = char(X.);
IND = strfind(X1,'F-Output-1');
int=[10,double('*FILE FORMAT, ASCII '),10,double('*NODE FILE'),10,'U',10];
String=char(int);
STRING= strcat(X1(1:IND+14),int);
STRING=strcat(STRING,X1(IND+14:end));

fid2 = fopen([Dat_file_end,'_A2M.inp'],'wt') ;
fwrite(fid2,STRING) ;
fclose (fid2) ;

%%

S1='D:\temp\Delamination 2\A2M_GUI_Output';
cd(S1)

Script_delamination_A2M

S='D:\temp\Delamination 2';
cd(S)
%% defining time vector
fid = fopen([Py_file,num2str(k),'.py'],'rt') ;

```

```

Deltat = fread(fid) ;
fclose(fid) ;
Deltat1 = char(Deltat.') ;
IND = strfind(Deltat1,'initialInc=');
Deltat=Deltat(IND+11:end);
Deltat1 = char(Deltat.') ;
IND = strfind(Deltat1,',');
Deltat=Deltat(1:IND(1)-1);
Deltat1=char(Deltat. ');
Deltat=str2num(Deltat1);
t=0:Deltat:endtime;
%
%% U
A=U{1,1};
f=find(A(:,1)==13);
A=A(f,:);

% plot(t(2:end),A(:,3))
figure
%nodal displacement
A1=U{1,1};
f=find(A1(:,1)==15);
A1=A1(f,:);
plot(t(2:end),A1(:,2))

All_displacement(:,k)=A1(:,2)

%% This script is the same as before, it is done in order to consider the new force
if k~=1
    peaks1 = findpeaks(All_displacement(:,1));
    peaksk = findpeaks(All_displacement(:,k));
    max1=abs(max(peaks1(ceil(length(peaks1)/2):end)));
    maxk=abs(max(peaksk(ceil(length(peaksk)/2):end)));

    fid = fopen([Py_file,num2str(k),'.py'],'rt') ;
    X = fread(fid) ;
    fclose(fid) ;
    X1 = char(X.') ;
    IND = strfind(X1,'cf2');
    X1=X1(IND:end);
    IND2=strfind(X1,10);
    X1=X1(5:IND2(1)-3);
    Fk=str2num(X1);
    Fk1=Fk*max1/maxk;

    fid = fopen([Py_file,num2str(k),'.py'],'rt') ;
    X = fread(fid) ;
    fclose(fid) ;
    X1 = char(X.') ;
    Stringk=[X1(1:IND+3),num2str(Fk1),X1(IND+IND2-3:end)]

    fid2 = fopen([Py_file,num2str(k),'.py'],'wt') ;
    fwrite(fid2,Stringk) ;
    fclose (fid2) ;

%%

```

```

system(['abaqus cae ',abd,'=',Py_file,num2str(k),'.py & ']); %la & serve a non farlo andare in
loop

sw=true;
while sw
    % Pause Matlab execution in order for the lck file to be created
    pause(0.5);
    % While the lck file exists, pause Matlab execution. If it is
    % deleted, exit the while loop and proceed.
    while exist([Pari,'.txt'],'file')==2
        pause(0.1)
        % the log file has been created and Matlab halts in this loop.
        % Set sw to false to break the outer while loop and continue
        % the code execution.
        sw=false;
        break %it is necessary because the second while is a loop
    end
end
delete('pari.txt')
%% modifying the .inp file

fid = fopen([Dat_file_end,'.inp'],'rt') ;
X = fread(fid) ;
fclose(fid) ;

S1='D:\temp\delamination 2\A2M_GUI_Output'
cd(S1) ;

X1 = char(X.');
IND = strfind(X1,'F-Output-1');
int=[10,double('*FILE FORMAT, ASCII '),10,double('*NODE FILE'),10,'U',10];
String=char(int);
STRING= strcat(X1(1:IND+14),int);
STRING=strcat(STRING,X1(IND+14:end));

fid2 = fopen([Dat_file_end,'_A2M.inp'],'wt') ;
fwrite(fid2,STRING) ;
fclose (fid2) ;

%%

S1='D:\temp\Delamination 2\A2M_GUI_Output';
cd(S1)

Script_delamination_A2M

S='D:\temp\Delamination 2';
cd(S)

%% U
A=U{1,1};
f=find(A(:,1)==13);
A=A(f,:);

% plot(t(2:end),A(:,3))
figure

```

```
%nodal displacement
A1=U{1,1};
f=find(A1(:,1)==15);
A1=A1(f,:);
plot(t(2:end),A1(:,2))

All_displacement(:,k)=A1(:,2)
end

%% plotting
figure
y=1.5E-6*sin(900.*t(1:end-1));
y=y';
plot(t(2:end),[All_displacement,y], 'LineWidth',1)
legend('a','b','c','set')

end
```


Bibliography

- [1] Prof. K.Gopinath & Prof. M.M.Mayuram , *Machine Design II slides*, Indian Institute of Technology Madras
- [2] Shan-Tung Tu & Xian-Cheng Zhang, *Fatigue Crack Initiation Mechanisms*, East China University of Science and Technology, 2016
- [3] Anders Ekberg , *Fatigue crack propagation*, CHALMERS Solid Mechanics.
- [4] Miguel Patrício & Robert M.M. Mattheij, *Crack Propagation Analysis*
- [5] Xiaobin Lin, B. Sci .. A1. Sci., *Fatigue crack growth*, University of Sheffield
- [6] Ronald Krueger, *Virtual crack closure technique: History, approach, and applications*, National Institute of Aerospace, Hampton, Virginia 23666
- [7] Wei Ding, *Delamination Analysis of Composite Laminates*, Graduate Department of Chemical Engineering and Applied Chemistry, University of Toronto
- [8] Prof. Giancarlo Genta , *Vibration dynamics and control*, Springer
- [9] Indrajit Chowdhury , *Computation of Rayleigh Damping Coefficients for Large Systems*, Indian Institute of Technology
- [10] Zhiqiang Song and Chenhui Su , *Computation of Rayleigh Damping Coefficients for the Seismic Analysis of a Hydro-Powerhouse*, Xi'an University of Technology
- [11] Fabrizio Magi , *Vibration fatigue testing for identification of damage initiation in composites*, University of Bristol
- [12] H. Thomas Hahn , *Composite Materials: Fatigue and Fracture*, ASTM Committee E-24 on Fracture Testing
- [13] Michael John Brennan , *Stiffness Nonlinearity in Structural Dynamics: Our Friend or Enemy?*, Springer